



HAL
open science

Ion outflow and escape in the Terrestrial Magnetosphere: Cluster Advances

Iannis Dandouras

► **To cite this version:**

Iannis Dandouras. Ion outflow and escape in the Terrestrial Magnetosphere: Cluster Advances. Journal of Geophysical Research Space Physics, 2021, 10.1029/2021JA029753 . hal-03357476

HAL Id: hal-03357476

<https://hal.science/hal-03357476>

Submitted on 29 Sep 2021

HAL is a multi-disciplinary open access archive for the deposit and dissemination of scientific research documents, whether they are published or not. The documents may come from teaching and research institutions in France or abroad, or from public or private research centers.

L'archive ouverte pluridisciplinaire **HAL**, est destinée au dépôt et à la diffusion de documents scientifiques de niveau recherche, publiés ou non, émanant des établissements d'enseignement et de recherche français ou étrangers, des laboratoires publics ou privés.

Ion outflow and escape in the Terrestrial Magnetosphere: Cluster Advances

Iannis Dandouras¹

¹Institut de Recherche en Astrophysique et Planétologie, Université de Toulouse / CNRS / UPS / CNES, Toulouse, France.

Corresponding author: Iannis Dandouras (Iannis.Dandouras@irap.omp.eu)

Key Points:

- Cluster has advanced our understanding of how the atmosphere slowly escapes to space and has revealed previously hidden escaping populations
- The outflowing ion populations cover a very wide energy domain, from cold plasma to energetic ions, and contain both light and heavy ions
- Ion outflow occurs during all activity levels, but it can increase by two orders of magnitude during extreme space weather events

Abstract

Cluster was the first mission in the terrestrial magnetosphere to involve four spacecraft in a tetrahedral configuration, providing three-dimensional measurements of the space plasma parameters. Cluster was also equipped with a very comprehensive instrumentation, allowing the measurement of the ion populations outflowing from the ionosphere, their circulation in the magnetosphere and their eventual escape to outer space. The observations of the outflowing and escaping ion populations performed by Cluster are reviewed and the most prominent results highlighted. These show the dominance in the magnetotail lobes of cold plasma outflows originating from the polar caps. For the energetic heavy ion outflow the cusps constitute the main source. Their transport and acceleration through the polar cap into the lobes and then into the plasma sheet has been characterized. The dependence of the polar outflow on the solar wind parameters and on the geomagnetic activity has been evaluated for both cold ion populations and heavy energetic ions. For the latter, outflow has been observed during all periods but an increase by two orders of magnitude has been shown during extreme space weather conditions. This outflow is adequate to change the composition of the atmosphere over geological time scales. At lower latitudes, the existence of a plasmaspheric wind, providing a continuous leak from the plasmasphere, has been demonstrated. The general scheme of the outflowing ion circulation in the magnetosphere or escape, and its dependence on the IMF conditions, has been outlined. However, several questions remain open, waiting for a future space mission to address them.

Plain Language Summary

The Earth's upper atmosphere is slowly escaping to space, either in the form of light electrically neutral atoms (mainly hydrogen), or in the form of ions (all species). The Cluster mission, launched in year 2000 and consisting of 4 spacecraft orbiting the Earth, has greatly advanced our understanding of how the ions are outflowing from the upper atmosphere, can be accelerated by the electric and magnetic fields present there, and can then eventually escape to outer space. The results show how this escape is highly sensitive to the level of solar activity and geomagnetic activity. Although escape occurs under all activity conditions, during space storms it dramatically increases, and during extreme space weather events this increase in the escape rate can be by almost two orders of magnitude. This escape, in the long-term (few billion years) is adequate to change the composition of the Earth's atmosphere.

1 Introduction

Understanding the evolution of planetary atmospheres, and particularly the evolution of the composition of Earth's atmosphere, is a major challenge. The Earth is a unique habitable body with life actually present, and that is strongly related to its atmosphere. However, the present atmospheric composition, following 4.5 billion years of evolution, is quite different from that of the primordial Earth (Kasting, 1993; Stüeken et al., 2020). The evolution of the terrestrial atmosphere is driven by its interactions with the planet's crust and oceans, the biological activity, the influx from space (e.g., meteors) and the atmospheric escape to space (Hunten et al., 1989; Yamauchi and Wahlund, 2007; Lammer et al., 2008, 2020; Avicé and Marty, 2020; Gronoff et al., 2020).

On Earth, where the gravitational escape velocity is 11.2 km s^{-1} , atmospheric escape in the form of neutral atoms concerns essentially hydrogen (Jeans escape, i.e. escape due to the thermal velocities of the atoms). Heavier species, such as oxygen and nitrogen, need to be

accelerated in order to reach escape velocities. Atmospheric escape of these heavier species, which constitute more than 99% of the mass of the atmosphere, thus occurs in the form of ions. The ions that outflow from the ionosphere are successively accelerated through a series of energization mechanisms and can eventually reach velocities above the gravitational escape velocity (Delcourt et al., 1993; Yau and André, 1997; Huddleston et al., 2005; Gronoff et al., 2020). Depending on the outflow trajectory, the interplanetary magnetic field conditions, the magnetospheric convection and the ion species, some of the outflowing ions can be re-injected into the inner magnetosphere, whereas some can completely escape (Ebihara et al., 2006; Haaland et al., 2012; Chappell, 2015; Yamauchi, 2019). Outflow from the ionosphere also plays an important role in the dynamics of the magnetosphere, by loading the magnetosphere with heavy ions (Kronberg et al., 2014; Yamauchi and Slapak, 2018).

Earth being the most extensively explored planet of our solar system, there have been several missions since the beginning of the space era studying the upper atmosphere / ionosphere and the magnetosphere and collecting data on the ion and neutral sources, circulation within the magnetosphere and losses to outer space (e.g. Chappell, 2015; Dandouras et al., 2020). However the Cluster mission, launched in 2000 (Escoubet et al., 2001), was the first one to involve four identical spacecraft in a tetrahedral configuration, providing thus three-dimensional measurements of the space plasma parameters.

In this paper we review some of the observations of outflowing and escaping ion populations, performed by Cluster in the magnetosphere during the past 20 years. The scope is not to provide an exhaustive list of the Cluster observations, but to highlight some of the most prominent results provided by the mission in the field of terrestrial ion outflow and escape.

2 Instrumentation

The Cluster mission is based on four identical spacecraft launched into similar elliptical polar orbits with an initial perigee at about $4 R_E$ and an apogee at $19.6 R_E$ (Escoubet et al., 2001, 2015). This nominal orbit allows Cluster to traverse the inner magnetosphere, from south to north during every perigee pass, and then fly along the open magnetic field lines of the polar cap and/or the cusp towards the magnetotail or the dayside magnetosphere, depending on the epoch of the year (Dandouras et al., 2005, 2009). Due to the annual precession of the orbit Cluster is thus crossing the equator at all MLTs over a year.

Eleven experiments onboard each spacecraft allow a wide set of measurements of the plasma parameters (particles and fields). Among them, of particular interest for detecting escaping ion populations are the Cluster Ion Spectrometer (CIS), the high-energy instrument Research with Adaptive Particle Imaging Detectors (RAPID), the Electric Field and Wave experiment (EFW) and the Whisper of High frequency and Sounder for Probing Electron density by Relaxation (WHISPER) experiment.

The Cluster Ion Spectrometer experiment consists of two complementary ion sensors, the Composition and Distribution Function analyzer (CODIF) and the Hot Ion Analyzer (HIA). CODIF is a time-of-flight mass spectrometer that gives the ion composition with a $22.5^\circ \times 22.5^\circ$ angular resolution in the $\sim 0 - 40$ keV/e energy range and with a $\Delta E/E \approx 16\%$ energy resolution and an $m/\Delta m \approx 5 - 7$ mass resolution. HIA offers a better angular resolution ($5.6^\circ \times 5.6^\circ$) and covers the ~ 5 eV/e – 32 keV/e energy range with a $\Delta E/E \approx 18\%$ energy resolution, but without mass discrimination. The CIS experiment is thus capable of measuring the full three dimensional

ion distribution functions of the major ion species, from thermal energies up to about 40 keV/e, with a one-spacecraft-spin (4-second) time resolution (Rème et al., 2001).

The RAPID experiment is an imaging spectrometer for high-energy ions and electrons on board the four Cluster spacecraft, providing the complete particle parameters, i.e; velocity and atomic mass number, over an energy range from ~ 30 keV up to 1.5 MeV (Wilken et al., 2001).

EFW uses two pairs of spherical probes deployed on wire booms in the spin plane to measure the potential of the spherical probes relative to the spacecraft and the corresponding electric field. These measurements provide also the spacecraft potential, which is a weak function of the plasma density (Gustafsson et al., 2001).

WHISPER is a sounder experiment which in its active mode unambiguously identifies the electron plasma frequency, which is directly related to the total electron density. (Décréau et al., 2001). The electron plasma frequency can also be inferred from the WHISPER passive measurements by estimating the low frequency cut-off of natural plasma emissions.

Magnetic field topology information and particle pitch-angle distributions are deduced from the Cluster Fluxgate Magnetometer (FGM) instrument (Balogh et al., 2001).

Active spacecraft control, which is essential for keeping the spacecraft potential low in tenuous plasma environments so as to allow the detection of low-energy ions by the particle detection instruments, is provided on Cluster by the operation, during selected periods, of the Active Spacecraft Potential Control (ASPOC) instrument (Torkar et al., 2001).

3 Sources and outflow paths of escaping populations

The ions that flow out from the high-latitude ionosphere into the magnetosphere include:

- Ions upwelling from the polar cap, where the ambipolar electric field accelerates the ions upward along open magnetic field lines and they constitute the polar wind (Chandler et al., 1991; Abe et al., 1993, 2004; Schunk, 2000).
- Ions from the polar cleft and the cusp, accelerated upwards through multistep processes (Horwitz and Lockwood, 1985; André et al., 1990).
- Ion beams accelerated in the auroral zone (Shelley et al., 1982; Hultqvist et al., 1988; André and Yau, 1997; Yau and André, 1997).

The trajectories of these upwelling ions are generally tailward and curvilinear, and they can then follow transport routes either directly to the magnetosheath through the cusp, or through the plasma mantle, or through the lobes (Figure 1). The later can then either stream downtail, or get into the plasma sheet through convection (Chappell et al., 1987).

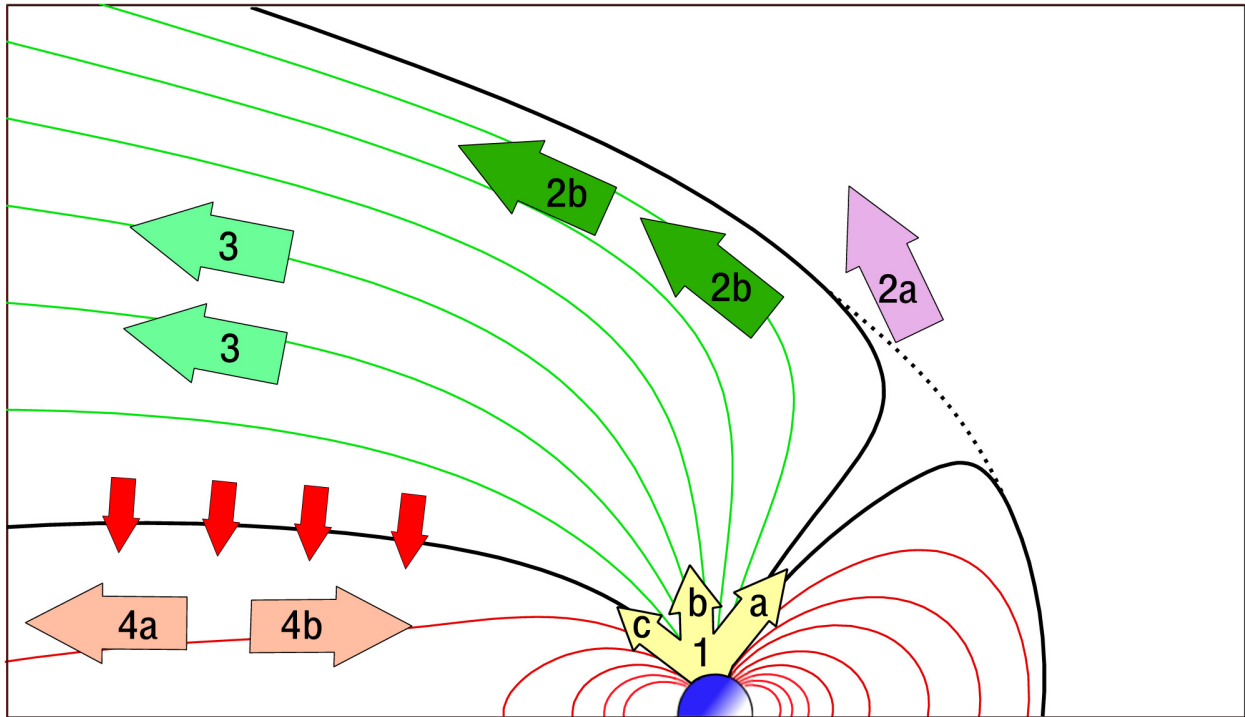


Figure 1. Sketch of the magnetosphere and of the upwelling ionospheric ions transport routes (northern hemisphere). The green and red magnetic field lines correspond to the open and closed magnetic field lines respectively. Ionospheric outflow is represented by yellow arrows. 1a – 1c, correspond to the cleft ion fountain, the polar wind and the auroral night zone outflow, respectively. Atmospheric escape to the magnetosheath is represented by direct escape from the cusp (2a, purple) and via the plasma mantle (2b, dark green). Lower energy ions fill the lobes (3, light green), and then feed the plasma sheet (red arrows), where both tailward and earthward transports take place (4a and 4b, beige). From Slapak and Nilsson (2018).

At equatorial latitudes the plasmasphere (Figure 2) constitutes another source of plasma release to the outer magnetosphere and eventual escape to the interplanetary medium (Lemaire, 2001; Borovsky et al., 2014).

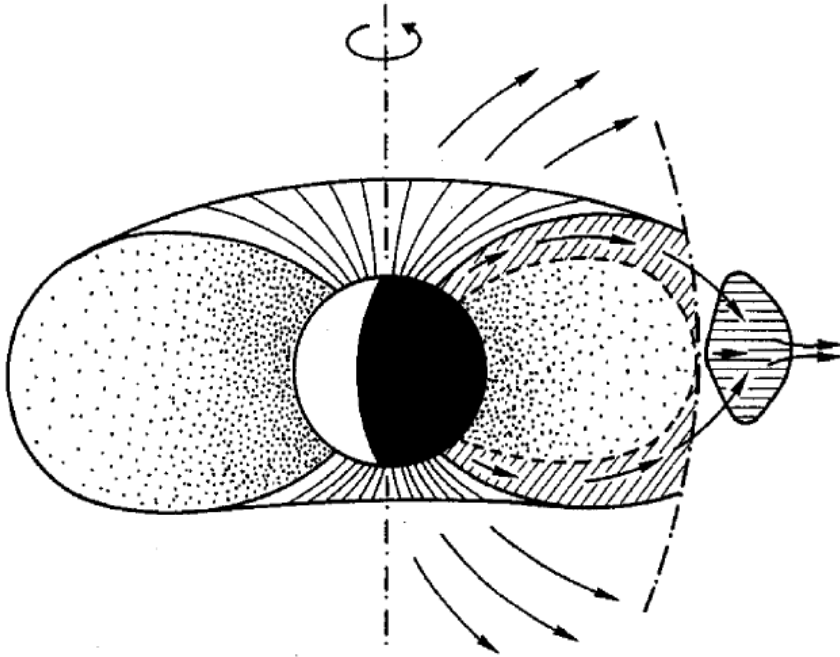


Figure 2. Sketch of a plasma element detachment from the plasmasphere, as a consequence of enhanced magnetospheric convection. From Lemaire (2001).

An additional reservoir for plasma escape from the inner magnetosphere, at equatorial latitudes, is the ring current. Escape from the ring current occurs either through the production and outwards emission of energetic neutral atoms (ENAs), which are the result of charge exchange interactions between singly charged trapped energetic ions and exospheric neutral atoms (Roelof, 1987; Ilie et al., 2013), or through ion leakage across the magnetopause during their drift around the Earth, also called magnetopause shadowing (Sibeck et al., 1987; Blanc et al., 1999). Escape from the ring current is however weaker, compared to the high-latitude ionosphere and to the plasmasphere.

3.1 Cusp outflow

In one of the early studies following Cluster launch, Bouhram et al (2004) took advantage of the multi-spacecraft configuration of Cluster in order to analyze the spatial and temporal coherence of O^+ ion outflow from the dayside cusp / cleft. The configuration of the tetrahedron, formed by the four spacecraft in 2001 when crossing the cusp / cleft, provided time delays between spacecraft of about 4 to 35 minutes, depending on the spacecraft pair considered (Figure 3). 18 outflow events in this period were analyzed using CIS data, for which O^+ velocities and outflow fluxes were calculated, and were then compared between spacecraft and cross-correlated to quantify the degree of coherence in the outflow for each event.

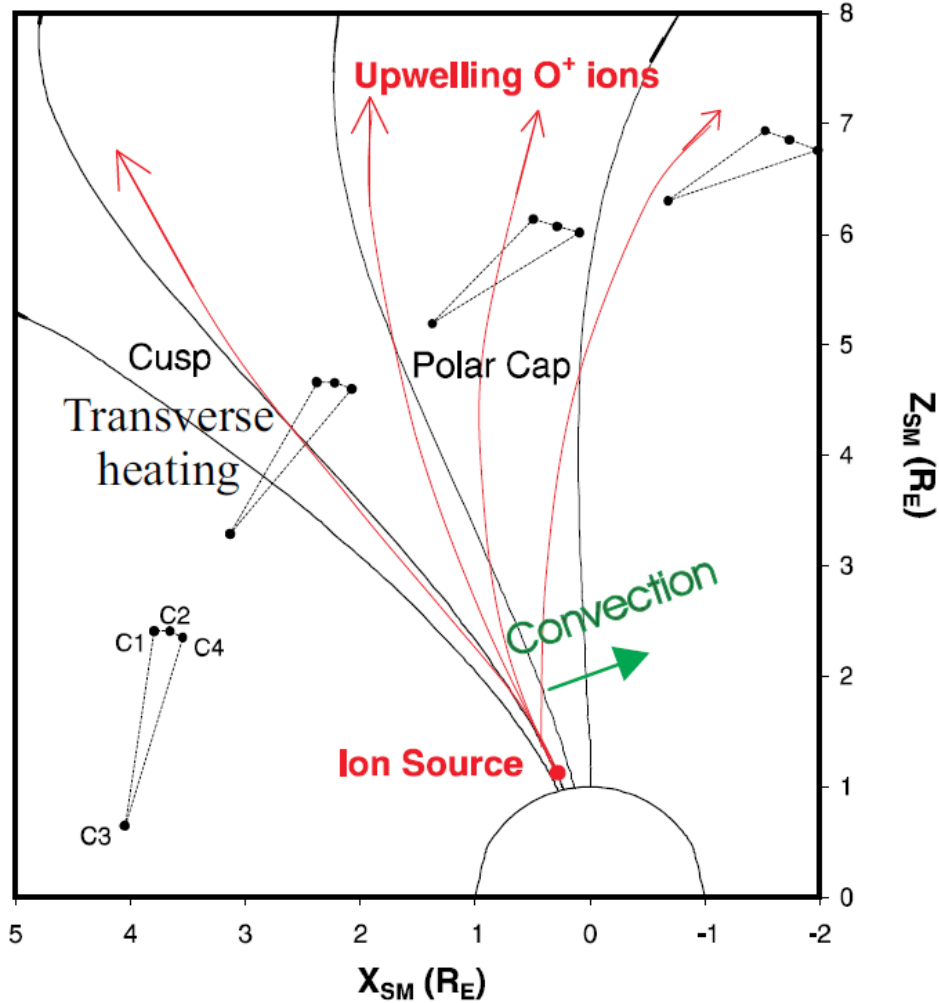


Figure 3. Schematic of the Cluster orbit configuration (spacecraft C1 – C4) in the cusp, dayside auroral and polar cap regions between July and November 2001. From Bouhram et al. (2004).

These multi-point observations provided, for the first time, direct evidence of non-stationary processes in the O^+ transport. The observed outflows were temporally variable, on a time scale of a few minutes. The convection electric fields varied on time scales that were much faster than the time of flight of the ions to reach the Cluster altitudes (3.5 to 6.5 R_E). Thus, although dayside outflows are a permanent feature, the observations showed that steady-state conditions are never achieved. The global outflow rate was however found to be more stable and depending mainly on the dynamic pressure of the solar wind.

The fate of these outflowing O^+ ions after they leave the cusp, and in particular how they are further accelerated and transported to the plasma sheet, has been studied in a series of two papers by Kistler et al. (2010) and Liao et al. (2015). These studies took advantage of the Cluster orbit which, a few months per year, can cross the cusp, then continue over the polar cap into the lobe and then it enters into the plasma sheet, allowing the tracking of the evolution of the O^+ populations in these regions along the same orbit by using the CIS instrument data. Kistler et al.

(2010) analyzed the outflowing O^+ transport during geomagnetic storms, and showed how it is transported across the polar cap into the lobes and then enters into the plasma sheet, where it is heated and becomes more isotropic. Liao et al. (2015) analyzed the distribution functions of the outflowing O^+ ions over the cusp, under various activity conditions, and compared them to the distribution functions of streaming energetic O^+ ions acquired in the lobes, at $\sim 20 R_E$ distances. The analysis showed that during non-storm times the observed changes in the beam velocity can be explained with the velocity filter effect, the outflow from the cusp being dispersed as a function of its velocity as it is transported to the tail. As the spacecraft then access different spatial regions along the orbit, they measure different beam velocities. These results suggest that, during non-storm times, there is no evidence of significant acceleration from the cusp to the polar cap and then to the tail lobes. Nevertheless, during geomagnetic storms ion acceleration is required to explain the streaming O^+ distributions observed in the lobes. In the plasma sheet boundary layer (PSBL), however, the streaming O^+ distribution functions, with energies from 500 eV to 7 keV, require a strong velocity increase during both storm and non-storm times, indicating that acceleration has taken place. Part of this energy increase is perpendicular to the magnetic field and is due to an enhanced $\mathbf{E} \times \mathbf{B}$ convection velocity. Another part of the energization is resulting from acceleration parallel to the magnetic field, due to either nonadiabatic acceleration of the large gyroradii O^+ ions at the PSBL or due to wave heating.

3.2 Open polar region outflow

The outflow and the energization of O^+ ions above the polar caps has been studied in a series of papers by Nilsson et al. (2006, 2008a, 2008b, 2012).

In a statistical study of hydrogen and oxygen ion outflow, using Cluster CIS data obtained at high altitudes ($5 - 12 R_E$) above the polar cap and covering 3 years of data (2001 – 2003), Nilsson et al. (2006) showed that these two species are energized to nearly the same velocity. Figure 4 shows a typical observation of an outflowing H^+ and O^+ beam, observed by Cluster above the polar cap, as those analyzed by Nilsson et al. (2006). As their analysis showed, the temperature of the outflowing O^+ beams increases strongly with altitude and as the associated magnetic field intensity decreases. The O^+ perpendicular temperature typically increases from a few ~ 10 eV, at altitudes with 150 nT magnetic field intensity, to a few keV at those with 50 nT. The H^+ and O^+ perpendicular temperatures appear to be coupled, but with a stronger increase for the O^+ temperature. The parallel bulk velocities of H^+ and O^+ appear also to be coupled. The thermal velocity of O^+ is however always below that of H^+ , and at the highest observed temperatures (and thus altitudes) there is a difference by a factor of about 3 between the temperatures of these two ion species. The analysis by Nilsson et al. (2006) suggests that there must be a parallel acceleration mechanism which provides a similar parallel velocity to the two ion species.

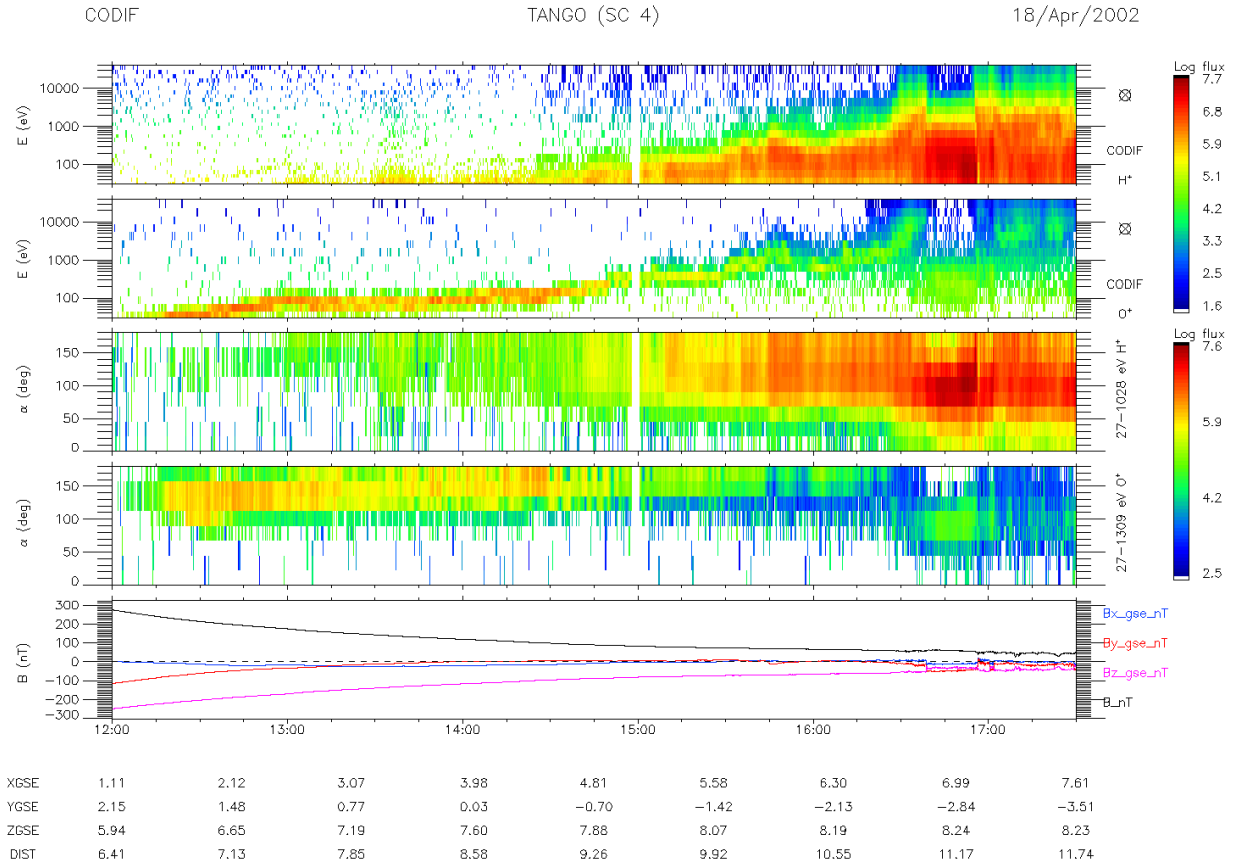


Figure 4. Cluster spacecraft 4 observation of an outflowing ion beam, detected by the CIS-CODIF instrument above the north polar cap during an outbound orbit. Top two panels: energy-time spectrograms for H^+ and O^+ ions, in particle flux units ($\text{ions cm}^{-2} \text{s}^{-1} \text{sr}^{-1} \text{keV}^{-1}$). Next two panels: pitch angle distributions for H^+ and O^+ ions, in the 27 – 1028 and 27 – 1309 eV energy ranges respectively, also in particle flux units. The outflowing ions population corresponds to the dominant $>90^\circ$ pitch angle population. Bottom panel: magnetic field measured by the FGM instrument, total and in GSE components. The spacecraft GSE coordinates and geocentric distance appear at the bottom of the figure.

The nature of this acceleration mechanism was investigated in a following paper (Nilsson et al., 2008a), where it was shown that the centrifugal acceleration, caused by the curvature of the magnetic field-lines in the direction of the magnetospheric convection, is an important energization mechanism for the outflowing O^+ ions. This acceleration is often of the order of 10 m s^{-2} and can frequently reach 100 m s^{-2} .

The spatial distribution of the trajectories of the H^+ and O^+ ions outflowing from the polar cap, as well as how this distribution affects the ion heating and acceleration, was analyzed in the paper by Nilsson et al. (2012). These ions can either get energized up to several keV in the high-altitude cusp or in the mantle, or appear as cold ions streaming downtail in the magnetotail lobes. Figure 5 shows the H^+ and O^+ outflowing ion densities and bulk velocities that were obtained by Nilsson et al. (2012) by analyzing 3 years (2001 – 2003) of Cluster CIS data. The observations are best organized when the ion outflow paths are sorted in three categories: cusp, central polar cap and nightside polar cap. The cusp appears to be a region of intense wave activity and the

major source of the O^+ outflow. Most of this cusp O^+ outflow is sufficiently accelerated to finally escape to the interplanetary space. The polar cap source, on its side, is consistent with the typical outflow trajectories of the cold ions that are observed in the magnetotail lobes.

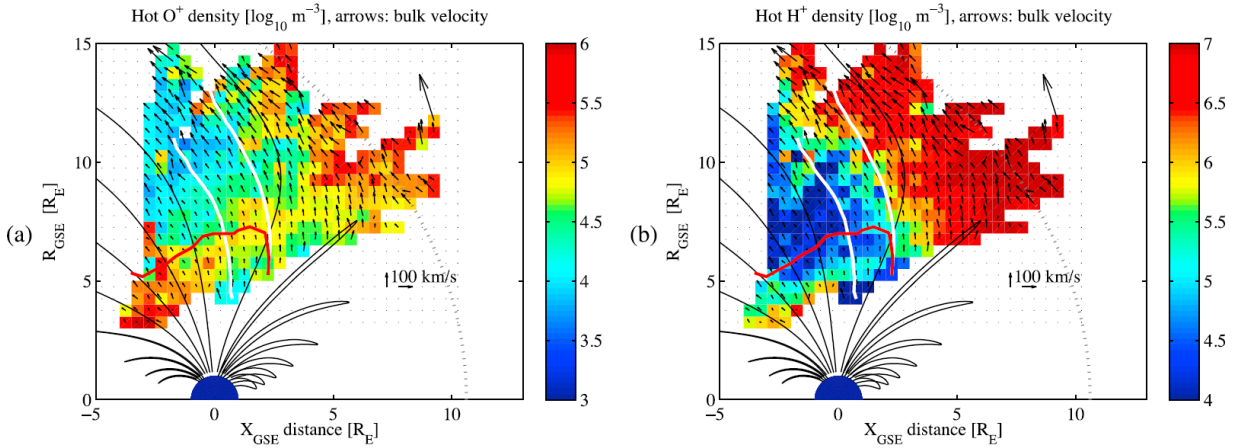


Figure 5. Densities ($\log_{10} \text{ m}^{-3}$) and velocities of (a) hot O^+ and (b) hot H^+ outflowing ions, shown in cylindrical GSE coordinates (R_E), where $R_{GSE} = \sqrt{Y_{GSE}^2 + Z_{GSE}^2}$. The two white lines correspond to two average ion flight trajectories bordering the central polar cap and the red line indicates a flight trajectory for cold ions subject to the average perpendicular bulk drift. From Nilsson et al. (2012).

3.3 Low-energy ion flow in the magnetotail lobes

One of the major contributions of Cluster in assessing ionospheric outflow has been the measurement of cold ions (of the order of a few eV in thermal energy) escaping downtail along the lobe magnetic field lines (Engwall et al., 2006, 2009). Spacecraft charging to potentials higher than the equivalent energy of these ions, as is the case in the tenuous magnetotail lobes when the active spacecraft control operation (ASPOC instrument) is not operating, can make these cold ion populations “invisible” to the particle detection instruments (Torkar et al., 2001; Rème et al., 2001; André et al., 2021). However, the supersonic flow of these downstreaming cold ions forms a wake behind the positively charged spacecraft when the bulk ion flow energy is higher than the ion thermal energy. This ion wake is then filled with subsonic electrons, creating a negative potential in the wake, which is then measured by the EFW double probe instrument, revealing this “hidden” cold ion outflow.

The method was first validated when comparing EFW electric field measurements and CIS RPA-mode (low-energy mode) ion measurements on two Cluster spacecraft, with the ASPOC active spacecraft potential control operating on Cluster spacecraft C4 and off on spacecraft C3, respectively (Engwall et al., 2006). The detection of an outflowing H^+ beam onboard spacecraft C4, where the ASPOC operation was reducing the spacecraft potential to 7 V, and the absence of detection onboard the closely spaced spacecraft C3, where the ASPOC was not operating and the spacecraft potential was varying between 40 V and over 60 V, allowed to confirm the identification of the beam by the EFW double probe measurements.

The ion wake method allowed Cluster to study cold ion outflow covering a much larger volume in magnetospheric regions, compared with previous missions such as Polar and Akebono

which were mostly limited to polar regions and to smaller geocentric distances (Figure 6a). The statistical analysis of the Cluster EFW data using the ion wake method, for the data acquired in the magnetotail during the 2002 tail season (Figure 6b), has shown that cold plasma outflows constitute a major part of the net loss of matter from the Earth (Engwall et al., 2009; André et al., 2015). Cold ions dominate in both flux and density in the distant magnetotail lobes. The total loss of cold hydrogen ions from the planet is inferred to be of the order of 10^{26} s^{-1} (Engwall et al., 2009), which is larger than the previously observed more energetic outflow (Peterson et al., 2001). This suggests that cold plasmas around the Earth, and planetary bodies in general, are much more important than previously anticipated.

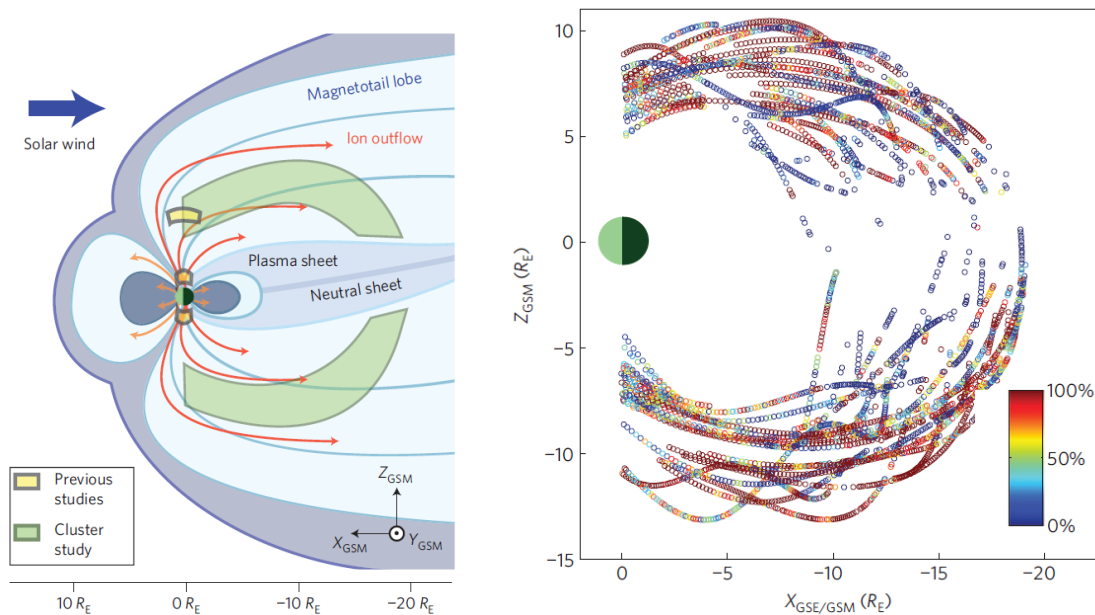


Figure 6. Left: Statistical studies of outflows from the polar ionosphere with energies of the order of 10 eV have previously been conducted close to the Earth, at high altitudes ($\sim 8 R_E$) by Polar and at low altitudes (5 000 – 10 000 km) by Akebono and Polar. The Engwall et al. (2009) study with Cluster covered a much larger volume in regions of the magnetosphere, where these ions had been previously invisible. Right: Parts of Cluster orbits with geocentric distances over $5 R_E$, for which the wake method to detect cold ions was used. Each point in the graph corresponds to 10 min of data and the color shows the relative occurrence of cold ions. The data are from Cluster spacecraft C3 between July and October 2002. From Engwall et al. (2009).

3.4 Plasmaspheric outflows

Since the early days of magnetospheric research it has been known that plasma tongues can be wrapped around the plasmasphere, shoulders or plasma irregularities can be formed and then they can be detached from the main body of the plasmasphere and form plumes (e.g. Lemaire, 1974, 2001). Plasmaspheric plumes are associated with active periods and with fluctuations of the convective large-scale electric field, governed by solar wind conditions.

Cluster was the first mission to provide a meridian view of the plasmaspheric density, by the way of four orbital sweeps as the four spacecraft cross the plasmasphere near perigee, at around $4 R_E$, from the southern to the northern hemisphere. Each spacecraft has been providing a density profile along its track. The total plasma density is obtained from the WHISPER instrument, (Darrouzet et al., 2006, 2008, 2009), whereas ion composition is provided by the CIS instrument when operating in its RPA mode (Dandouras et al., 2005).

Figure 7, from Darrouzet et al. (2006), shows an example of the traversal of a plasmaspheric plume by the four Cluster spacecraft, where the local plasma density measured by each spacecraft is calculated from the electron gyro-frequency measured by the WHISPER instrument. The normal boundary velocity, projected on the magnetic equatorial plane, is then calculated using the four-point time-delay technique. The statistical analysis of plasmaspheric plumes (Darrouzet et al., 2008) has shown that they are a quite common feature, observed at 15% of the time in the outer region of the plasmasphere. A small increase of the geomagnetic activity is sufficient to produce plumes. They are observed mainly in the afternoon and pre-midnight MLT sectors, and sometimes in the morning MLT sector.

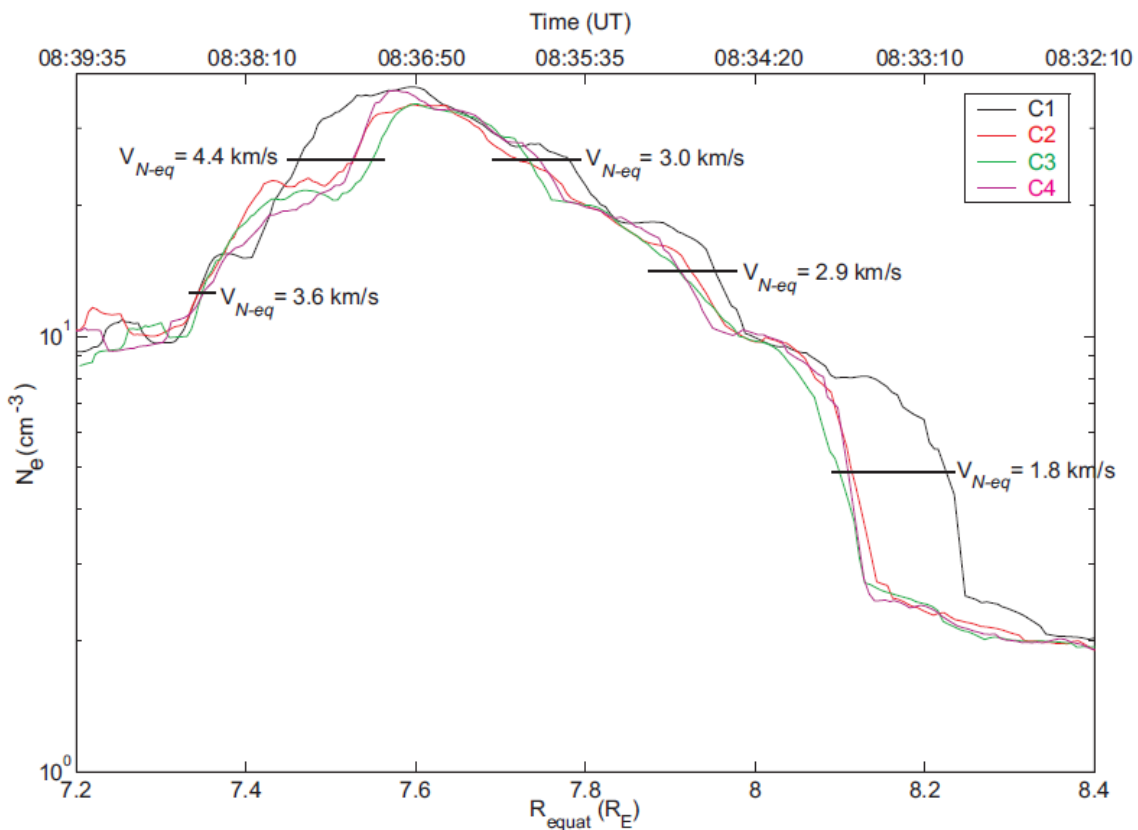


Figure 7. Example of electron density profiles as a function of R_{equat} , during the traversal of a plasmaspheric plume by the four Cluster spacecraft on 7 May 2002. The magnitude of the normal boundary velocity vectors $V_{N\text{-}eq}$ is derived from the time delays at different times during the crossing, projected onto the magnetic equatorial plane. From Darrouzet et al (2006).

Ion composition measurements in the outer plasmasphere, at $L \sim 4$, show a quasi-absence of O^+ ions (O^+ less than 4 % by number). Outside the main plasmasphere, however, a few low-energy O^+ observations occurred within plasmaspheric plumes originating from deeper in the plasmasphere and having an outward expansion velocity towards higher L -shells (Dandouras et al., 2005).

Are plumes the only mode for plasmaspheric material release to the outer magnetosphere? In 1992 an additional way for plasmaspheric material release to the outer magnetosphere was proposed: the existence of a plasmaspheric wind, steadily transporting cold plasmaspheric plasma outwards across the geomagnetic field lines, even during prolonged periods of quiet geomagnetic conditions (Lemaire and Schunk, 1992). The existence of this wind was proposed on a theoretical basis, as the result of plasma interchange motion driven by an imbalance between gravitational, centrifugal, and pressure gradient forces (André and Lemaire, 2006; Pierrard et al., 2009). Figure 8 shows the displacements of the plasma elements (the blue \times symbols) from their initial positions, initially aligned along the dipole magnetic field lines that are represented by the solid black lines. This outward radial transport, which is strongest at the geomagnetic equator, results in the plasmaspheric wind.

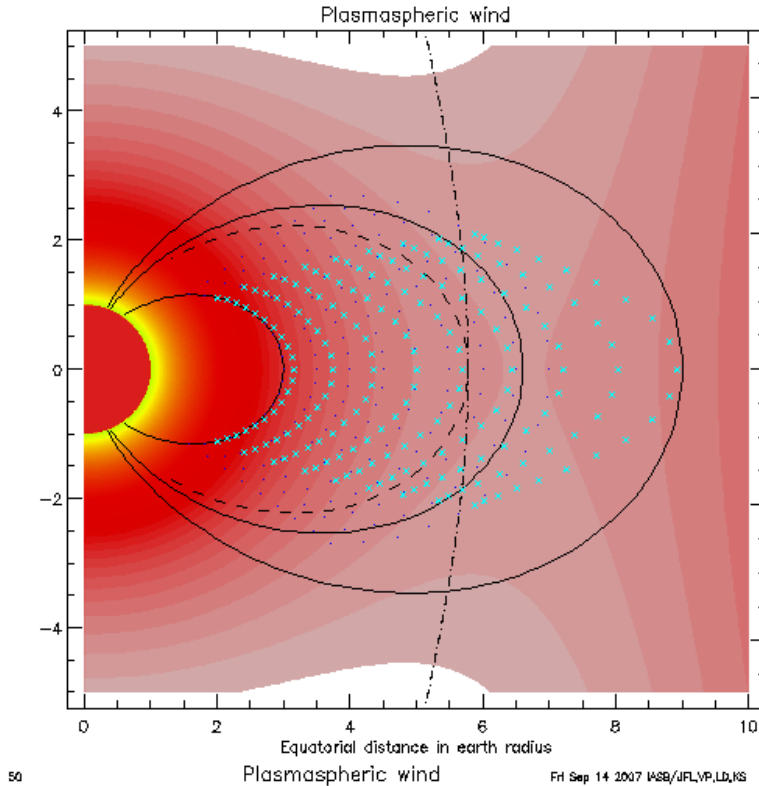


Figure 8. Plasmaspheric wind formation simulation, as the result of a plasma interchange motion driven by an imbalance between gravitational, centrifugal and pressure gradient forces. The simulation shows the displacements of the plasma elements (the blue \times symbols) from their initial positions, initially aligned along the dipole magnetic field lines that are represented by the solid black lines (Pierrard et al., 2009). Courtesy of Joseph F. Lemaire, Nicolas André and Viviane Pierrard.

Direct experimental evidence for the plasmaspheric wind was provided for the first time by the analysis of the ion distribution functions, acquired in the outer plasmasphere by the CIS experiment onboard Cluster (Dandouras, 2013). As shown in the example presented in Figure 9, the ion distribution functions obtained close to the magnetic equator reveal an imbalance between the outward and inward moving ions, both for H^+ and for He^+ ions, corresponding to a net outward flow. This outflow has been observed by Cluster during all analyzed events under quiet or moderately active magnetospheric conditions, in all MLT sectors, and it is consistent with the plasmaspheric wind. Calculations show that the observed radial outflow is of the order of 10^{26} ions s^{-1} in plasma loss from the plasmasphere. Similar winds should be observed also on other planets or astrophysical objects that are quickly rotating and have a magnetic field.

CIS–CODIF

C3 18/Mar/2002 10:52:00.

CIS–CODIF

C3 18/Mar/2002 10:52:00.

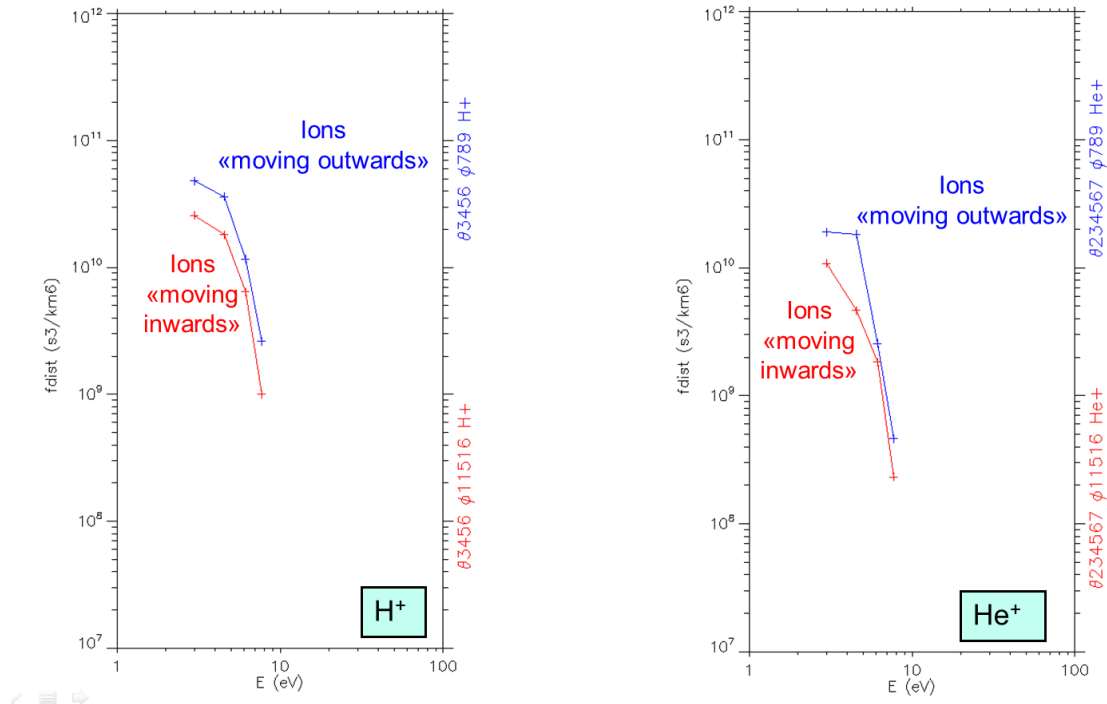


Figure 9. Partial distribution functions in the outer plasmasphere and close to the magnetic equator, corresponding to ions flowing radially outwards (blue plots) and to ions flowing radially inwards (red plots). Left panel is for H^+ ions and right panel is for He^+ ions. Ordinate axis is in phase space density units (ions $\text{s}^3 \text{ km}^{-6}$). The systematic imbalance between the outward and inward propagating ions reveals a net outward flow. From Dandouras (2013).

3.5 Ring current ion escape

Charge exchange interactions between the energetic ions and the exospheric neutrals, resulting in the ENA production and emission, is one of the main loss processes for the ring current ions (Keika et al., 2011). The emission of these ENAs can be used to form an image of the emitting region, mostly corresponding to the ring current. The IMAGE (Mitchell et al., 2000) and the TWINS (Goldstein and McComas, 2013) missions have been equipped with such ENA imagers. The retrieval of quantitative information on the parent ion populations from the ENA images, which contain an admixture of information on energetic ions and on cold neutral distributions, requires however image inversion techniques (C:son Brandt et al., 2002). The consistency between the retrieved energetic ion fluxes through the image inversions, and those really present locally in the ring current, has been validated for the first time by comparing inverted ENA images, obtained from the HENA imager onboard IMAGE, with the locally measured ion fluxes by the CIS instrument onboard Cluster (Vallat et al., 2004). Events were selected during which the Cluster spacecraft were within the ring current, in the field-of-view of the HENA imager, corresponding to both well-developed ring current conditions and to quiet geomagnetic conditions. This study showed quantitatively the consistency between the ion fluxes

deduced from the ENA image inversions and the fluxes measured locally, and demonstrated the complementarity of the two approaches, i.e. magnetospheric imaging and in-situ measurements.

Energetic heavy ion leakage across the magnetopause (i.e. magnetopause shadowing) has been studied by Marcucci et al. (2004). An event was selected during which two Cluster spacecraft were in the magnetosheath, skimming the magnetopause along the dawn-dusk meridian. Energetic (> 10 keV) O^+ ions were continuously observed by the CIS instrument onboard the two spacecraft, for almost 4 hours. While the O^+ density in the magnetosheath was almost constant, its velocity showed a strong dependence on the magnetic field orientation. The observations were best explained by a model considering that the oxygen ions cross the magnetopause outwards, due to their large gyroradii, and then taking into account the density gradient across the magnetopause and the convection in the magnetosheath. During southward magnetic field conditions, the oxygen ions while gyrating exit in the magnetosheath and then move tailward in the same direction as the magnetosheath convection, attaining high tailward velocities and thus escaping the geospace downtail. During northward magnetic field conditions, however, the particles that get in the magnetosheath move sunward while being convected tailward, so that the observed velocities are very low.

4 Outflow and escape dependence on external drivers and on activity conditions

4.1 Solar illumination control of ionospheric outflow above polar cap arcs

In order to study the solar illumination control of ionospheric outflow above polar cap arcs, Maes et al. (2015) analyzed the flux density, composition, and energy of outflowing H^+ and O^+ ions measured by the CIS instrument onboard Cluster. These ions are accelerated by quasi-static electric fields parallel to the magnetic field and associated with polar cap arcs. The analysis showed a clear transition at solar zenith angle (*SZA*) values between $\sim 94^\circ$ and $\sim 107^\circ$, with the O^+ flux higher above the sunlit ionosphere. This dependence on the illumination of the local ionosphere indicates that significant O^+ outflow occurs locally above the polar ionosphere. The same was also found for H^+ , but to a lesser extent. Solar illumination of the local polar ionosphere (particularly the F layer) is therefore considered as the main parameter controlling the outflow. Furthermore, the existence of two distinct regimes, for the sunlit and the dark polar ionosphere, suggests that a diurnal and seasonal variation for the total polar wind outflow may exist.

4.2 Outflow dependence on solar wind parameters

The modulation of the cold ion outflow (ions with energies lower than a few tens of eV) by the solar wind energy input to the magnetosphere was analyzed by Li et al. (2017), using the ion wake method (cf. section 3.3). The results showed that about 0.1% of the solar wind energy input is transferred to the kinetic energy of the cold ion outflow (mainly H^+ ions) at the topside ionosphere, with a typical hemispheric kinetic energy outflow rate on the order of 10^7 W. The energy transfer efficiency varies depending on the solar wind energy input parameter ε (Perreault and Akasofu, 1978), the solar EUV flux and the hemispheric dipole tilt angle. With increasing values of the ε parameter, both the median hemispheric outflow rate of cold ion kinetic energy and the median cold ion outflow rate increase by a maximum factor of 3. However, the energy transfer efficiency, from the solar wind to the cold ion outflow, decreases with increasing ε .

The solar wind and the EUV modulation of the more energetic ion outflow, and in particular of O^+ ($E > 40$ eV) ions, were studied by Schillings et al. (2019). The 2001 – 2005 CIS instrument data were used, and the analysis showed that the O^+ escape rate through the plasma mantle increases with increasing solar wind dynamic pressure. This dependence is shown schematically in Figure 10. It results in that the O^+ that will eventually escape through the plasma mantle increases, with the solar wind dynamic pressure, by about 2 orders of magnitude between the lowest and the highest dynamic pressure conditions. The IMF has also a clear influence on the O^+ escape, with an increase by a factor 3 between northward and southward IMF. The EUV flux, however, does not have a significant influence for the plasma mantle region. Therefore, atmospheric loss of heavy ions through the plasma mantle depends strongly on solar wind conditions but not on solar radiation.

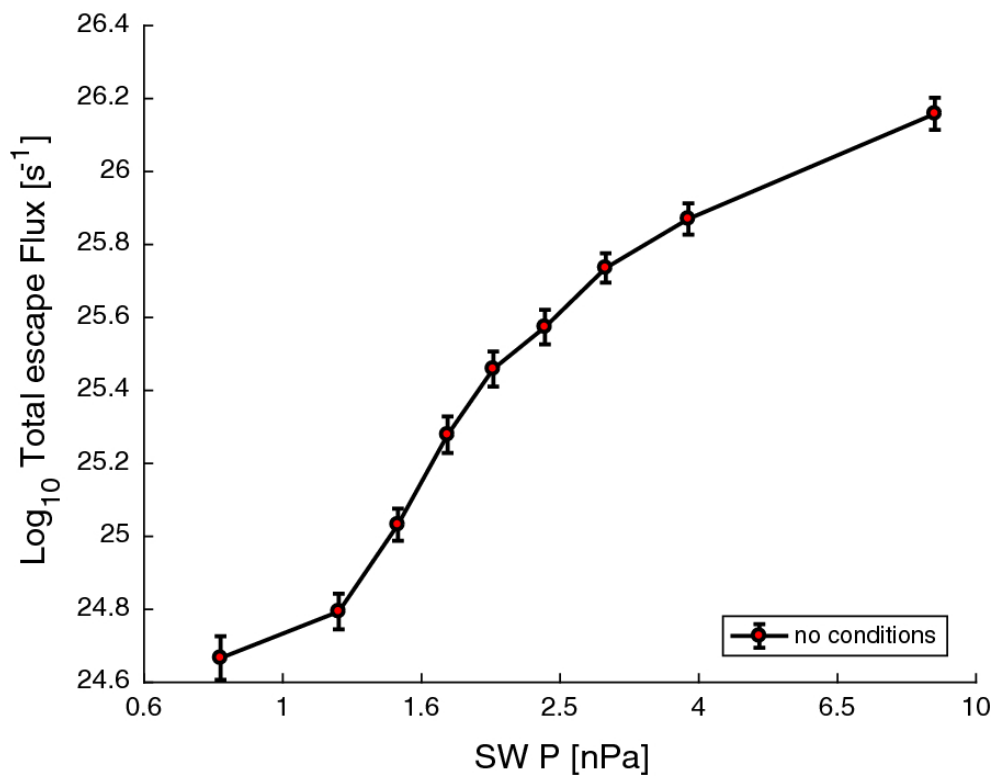


Figure 10. Solar wind dynamic pressure dependence of the energetic O^+ outflow through the plasma mantle: total O^+ escape flux as a function of the solar wind dynamic pressure for 9 equally distributed subsets. The error bars represent a 95% confidence interval. From Schillings et al. (2019).

4.3 Outflow dependence on geomagnetic activity

The dependence on the geomagnetic activity level of the O^+ escape through the dayside open polar region has been studied by Slapak et al. (2017). Two different escape routes of magnetospheric plasma have been investigated separately: the plasma mantle, and the direct escape from the dayside cusp to the magnetosheath (Figure 1, routes 2b and 2a respectively). The 2001 – 2005 CIS instrument data were analyzed (Figure 11a), and they show that the typical O^+

escape in high-latitude and high-altitude regions, via the plasma mantle and the dayside magnetosheath, increases exponentially as $\exp(0.45 Kp)$, cf. Figure 11b. This result is consistent with earlier observed O^+ outflow exponential dependences on Kp , but at lower altitudes and for Kp values up to ~ 6 , derived from the analysis of Dynamics Explorer (DE-1) data (Yau et al., 1988). It is also consistent with the exponential ion outflow flux dependence on the precipitating electron density, derived from the analysis of Fast Auroral Snapshot (FAST) Small Explorer data from the dayside high-latitude ionosphere (Strangeway et al., 2005).

As shown in Figure 11b, the dominant escape route is via the plasma mantle. Escape directly from the cusp into the dayside magnetosheath is smaller, but still significant.

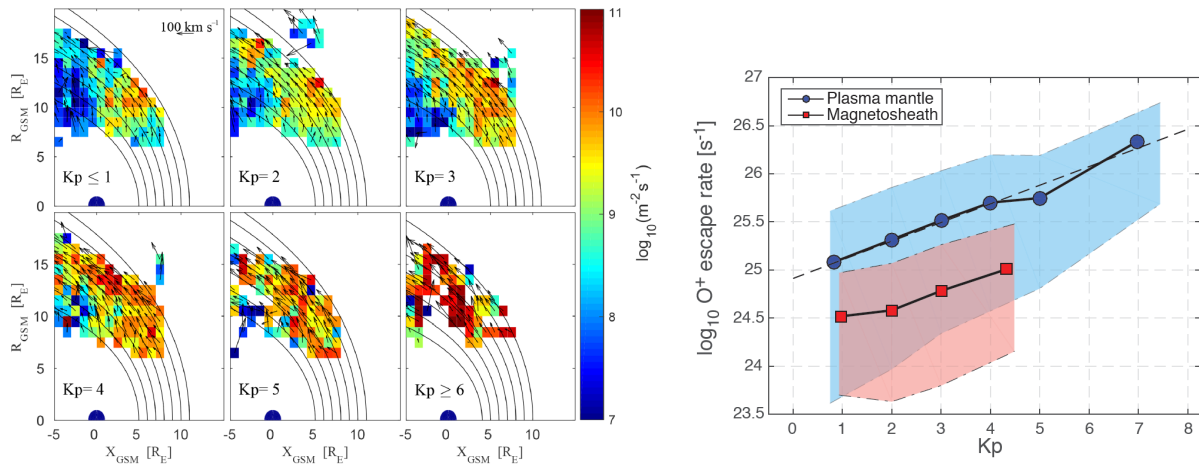


Figure 11. Left: The spatial distribution of the plasma mantle O^+ bulk flow flux in cylindrical coordinates, for periods of different geomagnetic conditions. The color bar defines the average flux intensity, and the arrows represent the average O^+ bulk velocity. Right: Average O^+ escape rates for the plasma mantle (solid black line and blue circles) and the dayside magnetosheath (solid black line and red squares) as a function of Kp . The dashed black line is a least squares fit to the logarithm of the average escape rates for the plasma mantle. The thin dot-dashed lines correspond to estimated upper and lower O^+ escape rates in the plasma mantle (blue area) and the magnetosheath (red), based on the highest and lowest flux values observed under the different geomagnetic conditions. From Slapak et al. (2017 and Corrigendum).

During extreme activity conditions ($Kp = 9$) the O^+ loss rate from the cusp and plasma mantle approaches values as high as 10^{27} s^{-1} , which are almost 2 orders of magnitude higher than those observed during typical average conditions (Nilsson, 2011). Considering that the young Sun was much more active than it is today, in terms of EUV radiation, faster solar wind, and a faster rotation with more active sunspots and a stronger IMF (Ribas et al., 2005; Güdel, 2020), and then assuming $Kp = 10$ four billion years ago and decreasing linearly with time, Slapak et al. (2017) integrated the O^+ loss over four billion years. It results in an estimated total O^+ escape, since the Earth was young until today, which is roughly equivalent to the amount of oxygen contained today in the terrestrial atmosphere. These results demonstrate the role of heavy ion escape in the evolution of the composition of the terrestrial atmosphere.

4.4 Outflow as a function of the solar cycle phase

The low-energy ion outflow during the solar cycle has been investigated by André et al. (2015) using the wake method. The 2001 (peak of solar cycle 23) to 2009 EFW instrument data were analyzed, and the results show that the low-energy ions usually dominate the density and the outward flux in the magnetotail lobes during all parts of a solar cycle. The global low-energy outflow is of the order of 10^{26} ions s^{-1} and it often dominates over the outflow of higher energy ions.

As shown in Figure 12, the outflow increases by a factor of 2 with increasing solar EUV flux during the solar cycle. This result, for the low-energy H^+ ion outflow from the polar caps, contrasts with the observed relative absence of sensitivity to the EUV flux for the heavy energetic ion outflow (mainly O^+ ions) through the plasma mantle region, reported by Schillings et al. (2019) and discussed here in section 4.2, revealing different underlying mechanisms.

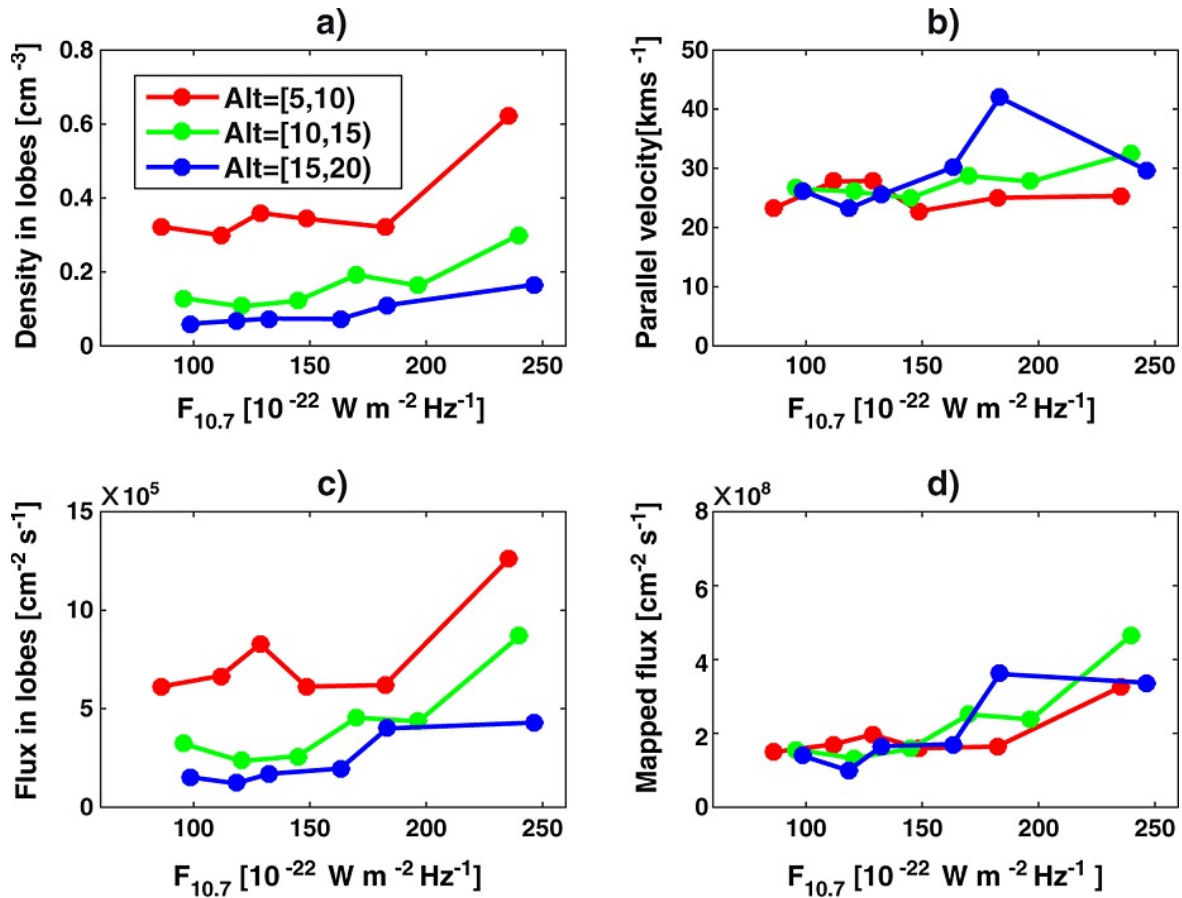


Figure 12. Low-energy ion outflows observed in the lobes, for three different altitude ranges (5 – 10, 10 – 15, and 15 – 20 R_E). (a) Density as a function of solar EUV radiation (estimated from the $F_{10.7}$ index). (b) Outward flow velocity parallel to the magnetic field. (c) Local flux in the magnetotail lobes. (d) Flux mapped to a 1000 km altitude. From André et al. (2015).

The increase of the low-energy ion outflow as a function of the solar EUV flux (André et al., 2015) is mainly due to the increased density of the outflowing population, whereas as shown in Figure 12b the outflow velocity does not vary substantially. The outflow is thus limited more by the available density in the ionospheric source than by the energy available in the magnetosphere to increase the ion outflow velocity.

4.5 Outflow of low-energy heavy ion beams observed during periods without substorms

Energetic heavy ion outflow, originating from the auroral oval, has usually been associated with high-activity periods (Daglis et al., 1990; Wilson et al., 2004). In order to examine whether the substorms are the only cause of ions flowing out of the auroral oval, Parks et al. (2015) analyzed H^+ , He^+ and O^+ ion flow data obtained in 2001 – 2002 by the CIS instrument at altitudes between $\sim 2 R_E$ and $\sim 10 R_E$. To identify periods with or without substorms, auroral images from the Wideband Imaging Camera (WIC) on the IMAGE spacecraft (Mende et al., 2000), together with the AE index, were then used. The results show evidence that auroral region ions do not escape only during substorms. During periods without substorms H^+ , He^+ and O^+ ions can be accelerated to moderate energies ($\sim 40 - 80$ eV), producing field-aligned beams. The escaping fluxes correspond then to a flow rate of $10^{19} - 10^{21}$ ions s^{-1} . Although these numbers are smaller than the cold ions escaping the polar cap, reported by Engwall et al., (2009) (10^{26} ions s^{-1} , cf. section 3.3), if we consider that the quiet auroral oval can persist for hours the total number of ions escaping here can be high in the long term.

On another study, Maggiolo et al. (2011) examined upward accelerated ion beams above the polar caps, occurring during periods of low geomagnetic activity. These beams, with energies up to a few keV and detected at altitudes between ~ 3 and $7.8 R_E$, are composed of H^+ and O^+ ions with varying proportions and appear as heated and accelerated polar wind ions. The spatial width of these beams, projected at an ionospheric altitude of 100 km, is generally less than 100 km, with a typical scale of about 30 – 40 km. They constitute an intermittent source active only during prolonged periods of northward IMF, appearing approximately 2 hours after the northward turning of the IMF. A southward turning of the IMF seems then to trigger their disappearance after roughly 20 minutes. The ion outflow, associated with these beams, can vary by two orders of magnitude.

4.6 Escape During the Extreme Space Weather Events

In order to quantify the ion outflow enhancements during major geomagnetic storms, Schillings et al. (2017) studied six such events that occurred between 2001 and 2004. These events fulfilled the criteria of $Dst < -100$ nT or $Kp > 7+$. The ion outflow data analyzed were provided by the Cluster CIS instrument. The results obtained showed a clear enhancement in the O^+ outflow in the polar cap region, scaled to an ionospheric altitude, by a factor of 3 to 83 during storm times. Such strong enhancements indicate that the entire magnetospheric circulation increases significantly during these extreme events. The upper limit for the scaled O^+ outflow was found in the Southern Hemisphere for the Halloween event (29 October 2003), with 2×10^{14} ions $m^{-2} s^{-1}$. The relative outflow enhancements, scaled to an ionospheric altitude, were found to vary with the Kp index consistently with the exponential law of Slapak et al. (2017). This corresponds to an almost 2 orders of magnitude increase for the total ion escape during extreme geomagnetic activity events, compared to quiet conditions (cf. Figure 11).

In a second paper, Schillings et al. (2018) investigated the consequences of severe space weather on the heavy ion outflow for an extreme event occurring during the declining phase of Solar Cycle 24. The event consisted in a series of X-flares and coronal mass ejections that occurred in early September 2017, and which produced a severe geomagnetic storm ($Kp \simeq 8$ and $Dst = -142$ nT). A succession of two interplanetary shocks hit the Earth within 24 hours and caused an equatorward motion of the cusp. The ionospheric O^+ outflow in the polar cap and cusp was estimated before and after the second shock, which was the one that initiated the main phase of the storm. The ionospheric O^+ outflow increased after the passage of the second shock by a factor 3 in the polar cap and by a factor 2 in the cusp. This relative enhancement of the O^+ outflow was lower than expected, compared to Schillings et al. (2017), but the initial value of O^+ outflow (before the second shock) was already as high as $\sim 10^{13} \text{ m}^{-2} \text{ s}^{-1}$. This unusually high ionospheric O^+ outflow was probably due to an enhancement after the first shock and a preheating of the ionosphere by the EUV flux, due to the multiple X-flares in the previous days.

4.7 Escape versus recirculation in the magnetosphere

As shown in Figure 1, the upwelling ions from the polar ionosphere that are accelerated to escape velocities do not systematically escape from geospace, but depending on the conditions and the outflow path can be re-injected into the inner magnetosphere. Haaland et al. (2012) analyzed a data set of 1 million records of electron density and plasma drift velocity measurements, corresponding to cold ion outflow observations in the magnetotail lobes (energies up to ~ 100 eV, mainly H^+ ions). The EFW probe potential measurements were used to obtain the electron density, whereas the outflow velocity and direction were calculated from measurements of the convection electric field (EDI instrument) and the observed spacecraft wake (EFW).

The results obtained by Haaland et al. (2012) show that the fate of the outflowing cold ionospheric plasma depends largely on the convection conditions in the magnetosphere and, to some extent, on the polar cap size (source area). The density and the outflow velocities to some extent do not respond to changes of the IMF on short timescales, whereas the convection is largely controlled by the IMF direction (Figure 13). During northward IMF and low geomagnetic activity conditions the outflow flux and velocity are low, and the outflowing ions are directly lost downtail. These directly escaping ions correspond to about 10% of the outflowing cold ions detected by Cluster at 6 – 20 R_E altitudes. During disturbed magnetospheric conditions however, typically associated with southward IMF, the outflowing cold light ions are transported towards the plasma sheet. From there they can eventually get injected towards the inner magnetosphere, get accelerated and contribute to the ring current formation.

It is noteworthy that, although these inward injected ions are not escaping directly, most of them will get lost ultimately through charge exchange interactions with exospheric neutral atoms and thus can escape the geospace as ENAs (Keika et al., 2011; Ilie et al., 2013).

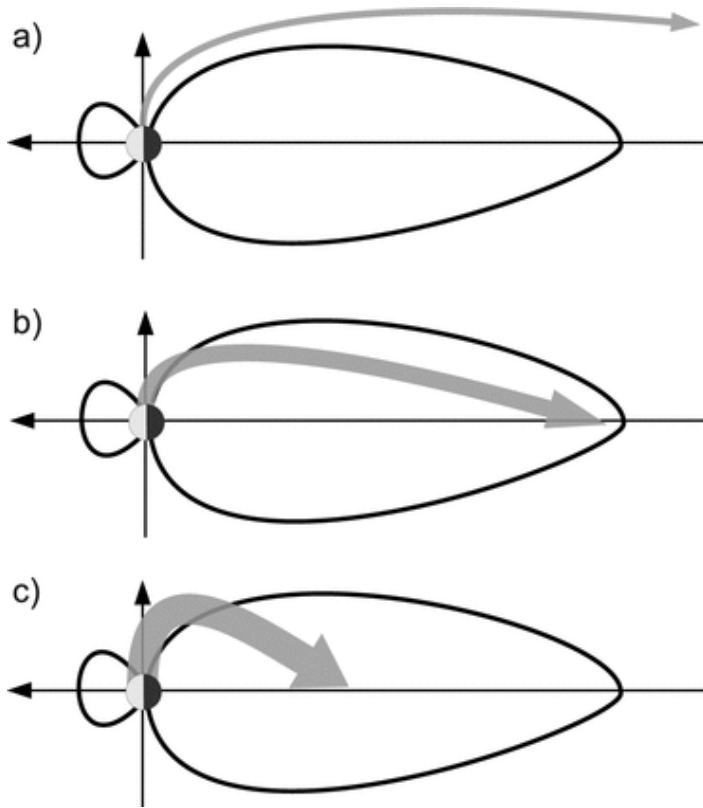


Figure 13. Typical trajectories of outflowing cold light ions for different disturbance levels. Thickness of arrows indicate flux level. (a) Northward IMF conditions and low geomagnetic activity. The outflow flux and velocity is low, and outflowing ions are directly lost downtail. (b) Low to intermediate convection: Outflowing ions are transported far downtail before reaching the plasma sheet. (c) Disturbed magnetospheric conditions, typically associated with southward IMF. Outflowing ions are transported to the plasma sheet closer to the Earth. From Haaland et al. (2012).

A review study of outflowing ions circulation in the magnetosphere and escape to outer space was undertaken by Yamauchi (2019). This study, largely based on Cluster CIS data, encompassed cold and suprathermal ions, providing a particular focus on the relevant behaviors of hot heavy ions in the inner magnetosphere. As shown, the majority of the outflowing ions becomes “hot” at higher altitudes, with much higher velocities than the escape velocity even for heavy ions. The immediate destination of these outflowing ionospheric ions varies from the plasmasphere, to the inner magnetosphere, the magnetotail, and the solar wind (magnetosheath, cusp, and plasma mantle). A significant number of them enter the plasma sheet, where some ions continue flowing anti-sunward, whereas other return towards the inner magnetosphere, where outflowing ions from different routes mix together. This results in the inner magnetosphere becoming a “zoo” of many different ion populations, either through direct supply from the ionosphere or through ions injected from the nightside plasma sheet, and subject to different energization mechanisms and transport routes. The principal destinations of the different types of outflowing ions are summarized in Figure 14.

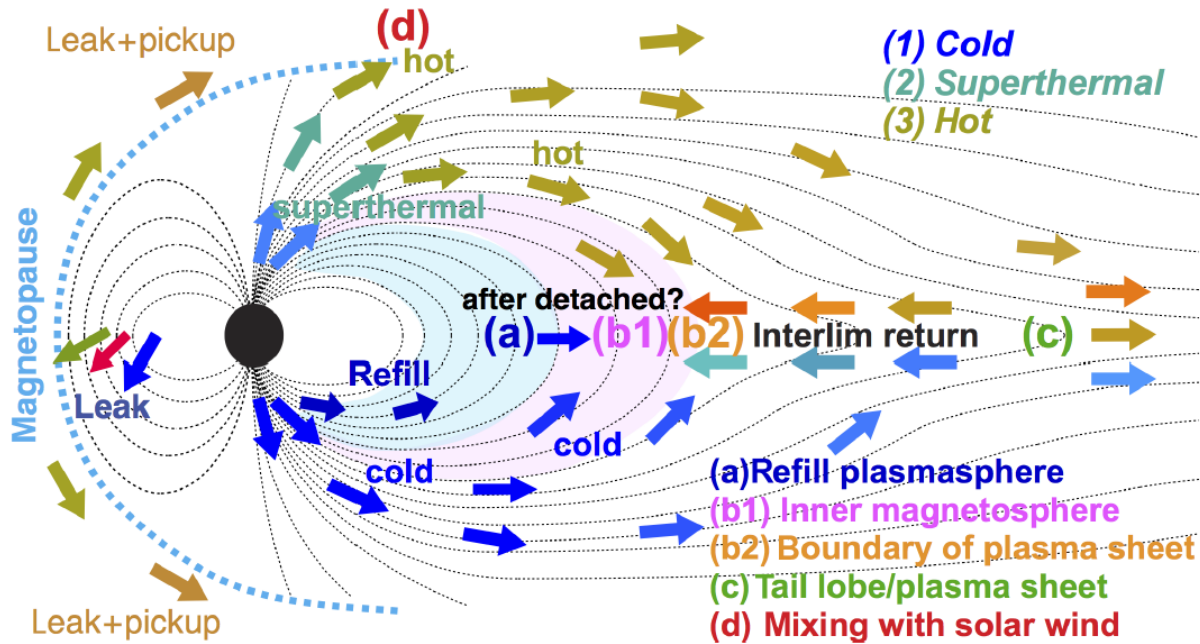


Figure 14. Schematic representation of the circulation of outflowing ions in the magnetosphere and their destination. From Yamauchi (2019).

As shown by Yamauchi (2019), the terrestrial ion outflow plays an important role in two issues that had been overlooked in the past:

- The mass-loading effect into the solar wind, which can explain quantitatively the energy conversion required to sustain the cusp current system.
- The influence on the atmospheric composition evolution over geological time scales, particularly after taking into account the more-active Sun and the higher solar wind pressure in the past.

5 Comparative studies with other planetary atmospheres

An enduring question in studying planetary atmospheres is whether an intrinsic planetary magnetic field plays a critical role in protecting the atmosphere from direct interaction with the solar / stellar wind, allowing the planet to retain a habitable atmosphere, or whether a magnetized planet could be more sensitive to atmospheric loss due to acceleration and escape of ions through the polar caps and cusp (Lundin et al., 2007; Gunell et al., 2018; Gronoff et al., 2020; Ramstad and Barabash, 2021).

In order to compare atmospheric O^+ outflow from Earth and Mars during a corotating interaction region (CIR) passage event, Wei et al. (2012) analyzed an event during which Sun, Earth, and Mars were approximately aligned. During the passage of the CIR, on 3 January 2008, Cluster was situated in the magnetotail lobe and the CIS instrument detected an enhanced O^+ outflow, fluctuating between 1×10^4 and 3×10^4 ions $cm^{-2} s^{-1}$. Oxygen ion outflow at Mars was measured by the Ion Mass Analyzer (IMA) instrument onboard Mars Express (Barabash et al., 2006). During the periapsis passes the instrument observed a series of spikes in the O^+ outflow

corresponding to $1 - 6 \times 10^7$ ions $\text{cm}^{-2} \text{s}^{-1}$, i.e. more than 1 order of magnitude higher than the pre-CIR level of 10^6 ions $\text{cm}^{-2} \text{s}^{-1}$. The O^+ outflow observed around the Martian magnetopause was probably the result of the pick-up process or of the momentum transfer mechanism (Dubinin et al., 2011). A comparison by the authors of these observations showed that, following a solar wind dynamic pressure increase by 2 – 3 nPa, the O^+ outflow flux at Mars increased by 1 order of magnitude higher than it increased at Earth. These results suggest that, under the conditions of the CIR event analyzed, the Martian O^+ outflow is more sensitive to solar wind dynamic pressure increases than the outflow from Earth, the terrestrial magnetic dipole apparently preventing a direct coupling between the solar wind kinetic energy and the planetary ions.

Successive observations from the Mars Atmosphere and Volatile Evolution (MAVEN) mission have confirmed the loss of substantial amounts of the Martian atmosphere to space, with H and O escape rates of the order of $\sim 2-3 \text{ kg s}^{-1}$ (Jakosky et al., 2018). It should be noted, however, that when comparing atmospheric escape rates between Earth and Mars, and their response to solar activity, extreme caution should be taken given the complexity of the various escape mechanisms involved, the different planetary masses and thus different escape velocities, and the different distances from the Sun of the two planets (Brain et al., 2017; Leblanc et al., 2018; Gronoff et al., 2020; Ramstad and Barabash, 2021).

6 Conclusions and open questions

Following 20 years of operation in space, the Cluster mission has strongly advanced our understanding of how the terrestrial upper atmosphere slowly escapes to space, and how this escape depends on the solar and the geomagnetic activity conditions. Several breakthroughs were made following the analysis of the data supplied by the instrumentation onboard these spacecraft. In particular:

- Cold plasma outflows, originating from the polar caps, dominate the magnetotail lobes during all parts of a solar cycle, constituting a previously “hidden” population. This low energy outflow increases by a factor of 2 with increasing EUV flux during the solar cycle.
- The role of the centrifugal acceleration in the energization of the ions upflowing from the polar caps has been demonstrated.
- The cusps constitute the main source of the energetic heavy ion outflow. The transport and acceleration of these ions through the polar cap into the lobes and then, depending on the IMF conditions, into the plasma sheet has been characterized.
- The existence of a plasmaspheric wind, which provides a continuous plasma leakage from the low-latitude plasmasphere and which was previously a theoretical conjecture, has been demonstrated.
- The dependence of the polar outflow on the solar wind parameters has been evaluated for both cold ion populations and heavy energetic ions. For the later, outflow has been observed during all periods but an increase in the outflow by two orders of magnitude between the lowest and the highest solar wind dynamic pressure conditions has been shown.
- The dependence of the polar outflow on the geomagnetic activity level has been evaluated and a logarithmic law established. During extreme activity conditions the

heavy ion loss is almost two orders of magnitude higher than during typical average conditions.

- The heavy ion loss measured by Cluster, when integrated over the past four billion years and considering the much more active young Sun, suggests a total O^+ loss comparable to the amount of oxygen contained today in the terrestrial atmosphere.
- The outflow of moderate energy ($\sim 40 - 80$ eV) light and heavy ions, forming beams that originate from the auroral oval, has been established even for periods without substorm activity.
- The general scheme of the circulation of outflowing ions in the magnetosphere or escape, and its dependence on the IMF conditions, has been outlined for both cold ions and for heavy energetic ions.
- Cluster light and heavy ion outflow observations cover almost two solar cycles, providing a data base suitable for comparative studies with other planetary atmospheres in our solar system, particularly during planet alignment along the same IMF spiral.

However, several questions concerning ion outflow and escape remain open.

The exact degree of plasma recirculation for each ion species, after it has left the ionosphere, versus direct or indirect escape, and its dependence on the solar and geomagnetic activity conditions, needs to be assessed more precisely.

The role of the plasmasphere in supplying plasma to the outer magnetosphere, either through plasmaspheric plumes release or through the plasmaspheric wind, and the ultimate fate of this plasma, that can eventually escape geospace, has to be accurately quantified.

But, most importantly, the exact composition of the escaping populations, and how it changes in response to the different driving conditions, is an open question. The moderate mass resolution of the CIS / CODIF ion mass spectrometer onboard Cluster ($m/\Delta m \approx 5 - 7$, cf. Rème et al., 2001) does not allow distinguishing the nitrogen ions from the oxygen ions. These two species together constitute more than 99% of the terrestrial atmosphere and they are both critical constituents of biomolecules such as amino acids and DNA / RNA. The biological activity on the Earth's surface is very sensitive to the atmospheric composition and a few percent change in the nitrogen / oxygen ratio, and thus in the water pH, can significantly affect biochemical reactions such as amino acid production, metabolism and photosynthesis (Servaites, 1977; Bada, 2013; Camprubí et al., 2019). The simultaneous presence of significant amounts of N_2 and O_2 in an atmosphere is chemically incompatible over geological timescales and thus it is considered as resulting from the biological activity (Lammer et al., 2019; Stüeken et al., 2020). Since atmospheric escape plays a critical role in the evolution of the composition of the atmosphere (Yamauchi and Wahlund, 2007; Airapetian et al., 2017), it is very important to assess how the composition of the escaping populations changes in response to different driver conditions, and in particular how the nitrogen / oxygen escape ratio changes as a function of the solar activity (Yau et al., 1993; Christon et al. 2002; Mall et al., 2002). These species have different dissociation energies, ionization energies, ionospheric chemistry and scale heights. Moreover, N^+ and O^+ ions injected in the magnetosphere play an essential role in the magnetospheric dynamics, particularly during periods of intense geomagnetic activity, resulting for example in different ring current decay time-profiles due to their different charge-exchange cross sections (Ilie and Liemohn, 2016; Lin et al., 2020).

The capacity to separate N^+ from O^+ ions (and also the corresponding molecular ions N_2^+ , NO^+ and O_2^+) over a broad energy range is thus an essential requirement for future magnetospheric missions, in order to understand how the composition of the escaping populations changes in response to the different driving conditions and how it can affect the atmospheric composition, and thus the habitability of the planet, over geological time scales.

Acknowledgments

The author is grateful to his numerous colleagues of the Cluster scientific community for the studies performed on ion outflow and escape, for which this paper presents a review and a synthesis of the main results. He also acknowledges the essential contribution of the technical teams that developed, prepared and operated the instruments onboard Cluster, and of the software engineers that developed the very efficient data processing tools.

French participation in the Cluster project has been supported in part by CNES.

All Cluster data are available at Cluster Science Archive, which can be accessed at: <https://csa.esac.esa.int/csa-web/>.

References

- Abe, T., Whalen, B. A., Yau, A. W., Horita, R. E., Watanabe, S., & Sagawa, E. (1993), EXOS D (Akebono) suprathermal mass spectrometer observations of the polar wind. *J. Geophys. Res.*, *98*, 11191– 11203, doi:10.1029/92JA01971
- Abe, T., Yau, A. W., Watanabe, S., Yamada, M., & Sagawa, E. (2004), Long-term variation of the polar wind velocity and its implication for the ion acceleration process: Akebono/suprathermal ion mass spectrometer observations. *J. Geophys. Res.*, *109*, A09305, doi:10.1029/2003JA010223
- Airapetian, V. S., Glocer, A., Khazanov, G. V., Loyd, R. O. P., France, K., Sojka, J., Danchi, W. C., & Liemohn, M. W. (2017), How Hospitable are Space Weather Affected Habitable Zones? The Role of Ion Escape. *Astroph. J. Lett.*, doi:10.3847/2041-8213/836/1/L3
- André, M., & Yau, A. (1997), Theories and Observations of Ion Energization and Outflow in the High Latitude Magnetosphere. *Space Sci. Rev.*, *80*, 27–48, doi:10.1023/A:1004921619885
- André, M., Crew, G. B., Peterson, W. K., Persoon, A. M., Pollock, C. J., & Engebretson, M. J. (1990), Ion heating by broadband low-frequency waves in the cusp/cleft. *J. Geophys. Res.*, *95*, 20809– 20823, doi:10.1029/JA095iA12p20809
- André, M., Li, K., & Eriksson, A. I. (2015), Outflow of low-energy ions and the solar cycle. *J. Geophys. Res.*, *120*, 1072–1085, doi:10.1002/2014JA020714
- André, M., Eriksson, A. I., Khotyaintsev, Y. V., & Toledo-Redondo, S. (2021), The spacecraft wake: Interference with electric field observations and a possibility to detect cold ions. *J. Geophys. Res.*, *126*, doi:10.1029/2021JA029493
- André, N., & Lemaire, J. F. (2006), Convective instabilities in the plasmasphere, *J. Atmosph. Sol.-Terr. Phys.*, *68*, 2, 213–227, doi:10.1016/j.jastp.2005.10.013

- Avice, G., and Marty, B. (2020), Perspectives on Atmospheric Evolution from Noble Gas and Nitrogen Isotopes on Earth, Mars & Venus. *Space Sci Rev*, 216, doi: 10.1007/s11214-020-00655-0
- Bada, J. L. (2013), New insights into prebiotic chemistry from Stanley Miller's spark discharge experiments. *Chem. Soc. Rev.*, 42, 2186
- Balogh, A., Carr, C. M., Acuña, M. H., Dunlop, M. W., Beek, T. J., Brown, P., Fornacon, K.-H., Georgescu, E., Glassmeier, K.-H., Harris, J., Musmann, G., Oddy, T., & Schwingenschuh, K. (2001), The Cluster Magnetic Field Investigation: overview of in-flight performance and initial results. *Ann. Geophys.*, 19, 1207–1217, doi:10.5194/angeo-19-1207-2001
- Barabash, S., Lundin, R., Andersson, H., et al. (2006), The Analyzer of Space Plasmas and Energetic Atoms (ASPERA-3) for the Mars Express Mission. *Space Sci. Rev.*, 126, 113–164, doi:10.1007/s11214-006-9124-8
- Blanc, M., Horwitz, J. L., Blake, J. B., Daglis, I., Lemaire, J. F., Moldwin, M. B., Orsini, S., Thorne, R. M., & Wolfe, R. A. (1999), Source and loss processes in the inner magnetosphere, *Space Sci. Rev.*, 88, 137–206, doi:10.1023/A:1005203817354
- Borovsky, J. E., Welling, D. T., Thomsen, M. F., & Denton, M. H. (2014), Long-lived plasmaspheric drainage plumes: Where does the plasma come from?. *J. Geophys. Res.*, 119, 6496– 6520, doi:10.1002/2014JA020228
- Bouhram, M., Klecker, B., Paschmann, G., Rème, H., Blagau, A., Kistler, L., Puhl-Quinn, P., & Sauvaud, J.-A. (2004), Multipoint analysis of the spatio-temporal coherence of dayside O⁺ outflows with Cluster. *Ann. Geophys.*, doi: 10.5194/angeo-22-2507-2004
- Brain, D. A., Bagenal, F., Ma, Y.-J., Nilsson, H., & Stenberg Wieser, G. (2016), Atmospheric escape from unmagnetized bodies. *J. Geophys. Res., Planets*, 121, 2364– 2385, doi:10.1002/2016JE005162
- Camprubí, E., de Leeuw, J.W., House, C.H. et al. (2019), The Emergence of Life. *Space Sci. Rev.*, 215, 56. Doi:10.1007/s11214-019-0624-8
- Chandler, M. O., Waite, J. H., & Moore, T. E. (1991), Observations of polar ion outflows. *J. Geophys. Res.*, 96, 1421– 1428, doi:10.1029/90JA02180
- Chappell, C. R. (2015), The Role of the Ionosphere in Providing Plasma to the Terrestrial Magnetosphere – An Historical Overview. *Space Sci. Rev.*, doi:10.1007/s11214-015-0168-5
- Chappell, C. R., Moore, T. E., & Waite, J. H. (1987), The ionosphere as a fully adequate source of plasma for the Earth's magnetosphere. *J. Geophys. Res.*, 92, 5896–5910, doi:10.1029/JA092iA06p05896
- Christon, S. P., Mall, U., Eastman, T. E., Gloeckler, G., Lui, A. T. Y., McEntire, R. W., & Roelof, E. C. (2002), Solar cycle and geomagnetic N⁺/O⁺ variation in outer dayside magnetosphere: Possible relation to topside ionosphere. *Geophys. Res. Lett.*, 29, doi:10.1029/2001GL013988
- Cson Brandt, P., Demajistre, R., Roelof, E. C., Ohtani, S., Mitchell, D. G., & Mende, S. (2002), IMAGE/high-energy energetic neutral atom: Global energetic neutral atom imaging of the plasma sheet and ring current during substorms. *J. Geophys. Res.*, 107, 1454, doi:10.1029/2002JA009307

Daglis, I. A., Sarris, E. T., & Kremser, G. (1990), Indications for ionospheric participation in the substorm process from AMPTE/CCE observations. *Geophys. Res. Lett.*, *17*, p. 57–60, doi:10.1029/GL017i001p00057

Dandouras, I. (2013), Detection of a plasmaspheric wind in the Earth's magnetosphere by the Cluster spacecraft. *Ann. Geophys.*, *31*, 1143–1153, doi:10.5194/angeo-31-1143-2013

Dandouras, I., Pierrard, V., Goldstein, J., Vallat, C., Parks, G. K., Rème, H., Gouillart, C., Sevestre, F., McCarthy, M., Kistler, L. M., Klecker, B., Korth, A., Bavassano-Cattaneo, M. B., Escoubet, P., & Masson, A. (2005), Multipoint observations of ionic structures in the Plasmasphere by CLUSTER-CIS and comparisons with IMAGE-EUV observations and with Model Simulations. *AGU Monograph: Inner Magnetosphere Interactions: New Perspectives from Imaging*, *159*, 23–53, doi:10.1029/159GM03, 2005

Dandouras, I., Cao, J., & Vallat, C. (2009), Energetic ion dynamics of the inner magnetosphere revealed in coordinated Cluster-Double Star observations, *J. Geophys. Res.*, *114*, A01S90, doi:10.1029/2007JA012757

Dandouras, I., Blanc, M., Fossati, L. et al. (2020), Future Missions Related to the Determination of the Elemental and Isotopic Composition of Earth, Moon and the Terrestrial Planets. *Space Sci Rev*, *216*, doi:10.1007/s11214-020-00736-0

Darrouzet, F., De Keyser, J., Décréau, P. M. E., Gallagher, D. L., Pierrard, V., Lemaire, J. F., Sandel, B. R., Dandouras, I., Matsui, H., Dunlop, M., Cabrera, J., Masson, A., Canu, P., Trotignon, J. G., Rauch, J. L., & André, M. (2006), Analysis of plasmaspheric plumes: CLUSTER and IMAGE observations. *Ann. Geophys.*, *24*, 1737–1758, doi:10.5194/angeo-24-1737-2006

Darrouzet, F., De Keyser, J., Décréau, P. M. E., El Lemdani-Mazouz, F., & Vallières, X. (2008) Statistical analysis of plasmaspheric plumes with Cluster/WHISPER observations. *Ann. Geophys.*, *26*, 2403–2417, doi:10.5194/angeo-26-2403-2008

Darrouzet, F., Gallagher, D.L., André, N. et al. (2009), Plasmaspheric Density Structures and Dynamics: Properties Observed by the CLUSTER and IMAGE Missions. *Space Sci Rev* *145*, 55–106, doi:10.1007/s11214-008-9438-9

Décréau, P. M. E., Ferreau, P., Krasnoselskikh, V., Le Guirriec, E., Lévêque, M., Martin, Ph., Randriamboarison, O., Rauch, J. L., Sené, F. X., Séran, H. C., Trotignon, J. G., Canu, P., Cornilleau, N., de Féraudy, H., Alleyne, H., Yearby, K., Mögensen, P. B., Gustafsson, G., André, M., Gurnett, D. C., Darrouzet, F., Lemaire, J., Harvey, C. C., & Travnicek, P. (2001), Early results from the Whisper instrument on Cluster: an overview. *Ann. Geophys.*, *19*, 1241–1258, doi:10.5194/angeo-19-1241-2001

Delcourt, D. C., Sauvaud, J. A., & Moore, T. E. (1993), Polar wind ion dynamics in the magnetotail. *J. Geophys. Res.*, *98*, 9155–9169, doi:10.1029/93JA00301

Dubinin, E., Fraenz, M., Fedorov, A., et al. (2011), Ion Energization and Escape on Mars and Venus. *Space Sci. Rev.*, *162*, 173–211, doi:10.1007/s11214-011-9831-7

Ebihara, Y., Yamada, M., Watanabe, S., & Ejiri, M. (2006), Fate of outflowing suprathermal oxygen ions that originate in the polar ionosphere. *J. Geophys. Res.*, *111*, doi:10.1029/2005JA011403

- Engwall, E., Eriksson, A.I., André, M., Dandouras, I., Paschmann, G., Quinn, J., & Torkar, K. (2006), Low-energy (order 10 eV) ion flow in the magnetotail lobes inferred from spacecraft wake observations. *Geophys. Res. Lett.*, *33*, L06110, doi:10.1029/2005GL025179
- Engwall, E., Eriksson, A., Cully, C. et al. (2009), Earth's ionospheric outflow dominated by hidden cold plasma. *Nature Geosci.*, *2*, 24–27, doi:10.1038/ngeo387
- Escoubet, C. P., Fehringer, M., & Goldstein, M. (2001), The Cluster mission. *Ann. Geophys.*, *19*, 1197–1200, doi: 10.5194/angeo-19-1197-2001
- Escoubet, C. P., Masson, A., Laakso, H., & Goldstein, M. L. (2015), Recent highlights from Cluster, the first 3-D magnetospheric mission. *Ann. Geophys.*, *33*, 1221–1235, doi:10.5194/angeo-33-1221-2015
- Goldstein, J., & McComas, D.J.(2013), Five Years of Stereo Magnetospheric Imaging by TWINS. *Space Sci. Rev.*, *180*, 39–70, doi:10.1007/s11214-013-0012-8
- Gronoff, G., Arras, P., Baraka, S., Bell, J. M., Cessateur, G., Cohen, O., et al. (2020), Atmospheric escape processes and planetary atmospheric evolution. *J. Geophys. Res.*, *125*, doi:10.1029/2019JA027639
- Güdel, M. (2020), The Sun Through Time. *Space Sci. Rev.*, *216*, doi: 10.1007/s11214-020-00773-9
- Gunell, H., Maggiolo, R., Nilsson, H., Stenberg Wieser, G., Slapak, R., Lindkvist, J., Hamrin, M., & De Keyser, J. (2018), Why an intrinsic magnetic field does not protect a planet against atmospheric escape. *Astronomy & Astrophysics*, *614*, doi:10.1051/0004-6361/201832934
- Gustafsson, G., André, M., Carozzi, T., Eriksson, A. I., Fälthammar, C.-G., Grard, R., Holmgren, G., Holtet, J. A., Ivchenko, N., Karlsson, T., Khotyaintsev, Y., Klimov, S., Laakso, H., Lindqvist, P.-A., Lybekk, B., Marklund, G., Mozer, F., Mursula, K., Pedersen, A., Popielawska, B., Savin, S., Stasiewicz, K., Tanskanen, P., Vaivads, A., & Wahlund, J.-E. (2001), First results of electric field and density observations by Cluster EFW based on initial months of operation. *Ann. Geophys.*, *19*, 1219–1240, doi:10.5194/angeo-19-1219-2001, 2001
- Haaland, S., Eriksson, A., Engwall, E., Lybekk, B., Nilsson, H., Pedersen, A., Svenes, K., André, M., Förster, M., Li, K., Johnsen, C., & Østgaard, N. (2012), Estimating the capture and loss of cold plasma from ionospheric outflow. *J. Geophys. Res.*, *117*, doi: 10.1029/2012JA017679
- Horwitz, J. L., & Lockwood, M. (1985), The cleft ion fountain: a two-dimensional kinetic model. *J. Geophys. Res.*, *90* (A10), 9749–9762, doi:10.1029/JA090iA10p09749
- Huddleston, M. M., Chappell, C. R., Delcourt, D. C., Moore, T. E., Giles, B. L., & Chandler, M. O. (2005), An examination of the process and magnitude of ionospheric plasma supply to the magnetosphere. *J. Geophys. Res.*, doi:10.1029/2004JA010401
- Hultqvist, B., Lundin, R., Stasiewicz, K., Block, L., Lindqvist, P.-A., Gustafsson, G., Koskinen, H., Bahnsen, A., Potemra, T. A., & Zanetti, L. J. (1988), Simultaneous observation of upward moving field-aligned energetic electrons and ions on auroral zone field lines. *J. Geophys. Res.*, *93*, 9765– 9776, doi:10.1029/JA093iA09p09765
- Hunten, D. M., Donahue, T. M., Walker, J. C. G., & Kasting, J. F. (1989), Escape of atmospheres and loss of water, in *Origin and evolution of planetary and satellite atmospheres*. University of Arizona Press, p. 386-422, 1989oeps.book..386H

- Ilie, R., & Liemohn, M. W. (2016), The outflow of ionospheric nitrogen ions: A possible tracer for the altitude-dependent transport and energization processes of ionospheric plasma. *J. Geophys. Res.*, *121*, 9250–9255, doi:10.1002/2015JA022162
- Ilie, R., Skoug, R. M., Funsten, H. O., Liemohn, M. W., Bailey, J. J., & Gruntman, M. (2013), The impact of geocoronal density on ring current development. *J. Atmos. Sol.-Terr. Phys.*, *99*, 92–103, doi:10.1016/j.jastp.2012.03.010
- Jakosky, B.M., Brain, D., Chaffin, M., Curry, S., Deighan, J., Grebowsky, J., Halekas, J., Leblanc, F., Lillis, R., Luhmann, J. G., Andersson, L., Andre, N., Andrews, D., Baird, D., Baker, D., Bell, J., Benna, M., Bhattacharyya, D., Bougher, S., Bowers, C., Chamberlin, P., Chaufray, J. -Y., Clarke, J., Collinson, G., Combi, M., Connerney, J., Connour, K., Correia, J., Crabb, K., Crary, F., Cravens, T., Crismani, M., Delory, G., Dewey, R., DiBraccio, G., Dong, C., Dong, Y., Dunn, P., Egan, H., Elrod, M., England, S., Eparvier, F., Ergun, R., Eriksson, A., Esman, T., Espley, J., Evans, S., Fallows, K., Fang, X., Fillingim, M., Flynn, C., Fogle, A., Fowler, C., Fox, J., Fujimoto, M., Garnier, P., Girazian, Z., Groeller, H., Gruesbeck, J., Hamil, O., Hanley, K. G., Hara, T., Harada, Y., Hermann, J., Holmberg, M., Holsclaw, G., Houston, S., Inui, S., Jain, S., Jolitz, R., Kotova, A., Kuroda, T., Larson, D., Lee, Y., Lee, C., Lefevre, F., Lentz, C., Lo, D., Lugo, R., Ma, Y. -J., Mahaffy, P., Marquette, M. L., Matsumoto, Y., Mayyasi, M., Mazelle, C., McClintock, W., McFadden, J., Medvedev, A., Mendillo, M., Meziane, K., Milby, Z., Mitchell, D., Modolo, R., Montmessin, F., Nagy, A., Nakagawa, H., Narvaez, C., Olsen, K., Pawlowski, D.; Peterson, W., Rahmati, A., Roeten, K., Romanelli, N., Ruhunusiri, S., Russell, C., Sakai, S., Schneider, N., Seki, K., Sharrar, R., Shaver, S., Siskind, D. E., Slipski, M., Soobiah, Y., Steckiewicz, M., Stevens, M. H., Stewart, I., Stiepen, A., Stone, S., Tenishev, V., Terada, N., Terada, K., Thiemann, E., Tolson, R., Toth, G., Trovato, J., Vogt, M., Weber, T., Withers, P., Xu, S., Yelle, R., Yiğit, E., & Zurek, R. (2018), Loss of the Martian atmosphere to space: Present-day loss rates determined from MAVEN observations and integrated loss through time. *Icarus*, doi:10.1016/j.icarus.2018.05.030
- Kasting, J.F. (1993), Earth's Early Atmosphere. *Science*, *259*(5097), 920-926, doi: 10.1126/science.11536547
- Keika, K., Brandt, P. C., Nosé, M., & Mitchell, D. G. (2011), Evolution of ring current ion energy spectra during the storm recovery phase: Implication for dominant ion loss processes. *J. Geophys. Res.*, *116*, doi:10.1029/2010JA015628
- Kistler, L. M., Mouikis, C. G., Klecker, B., & Dandouras, I. (2010), Cusp as a source for oxygen in the plasma sheet during geomagnetic storms. *J. Geophys. Res.*, *115*, doi:10.1029/2009JA014838
- Kronberg, E. A., Ashour-Abdalla, M., Dandouras, I., Delcourt, D. C., Grigorenko, E. E., Kistler, L. M., Kuzichev, I. V., Liao, J., Maggiolo, R., Malova, H. V., Orlova, K. G., Perroomian, V., Shklyar, D. R., Shprits, Y. Y., Welling, D. T., & Zelenyi, L. M. (2014), Circulation of Heavy Ions and Their Dynamical Effects in the Magnetosphere: Recent Observations and Models. *Space Sci. Rev.*, doi:10.1007/s11214-014-0104-0
- Lammer, H., Kasting, J. F., Chassefière, E., Johnson, R. E., Kulikov, Y. N., & Tian, F. (2008), Atmospheric Escape and Evolution of Terrestrial Planets and Satellites. *Space Sci. Rev.*, doi:10.1007/s11214-008-9413-5

- Lammer, H., Sproß, L., Grenfell, J.L., Scherf, M., Fossati, L., Lendl, M., & Cubillos, P.E. (2019), The Role of N₂ as a Geo-Biosignature for the Detection and Characterization of Earth-like Habitats. *Astrobiology*, 19, 927–950. doi:10.1089/ast.2018.1914
- Lammer, H., Scherf, M., Kurokawa, H. et al. (2020), Loss and Fractionation of Noble Gas Isotopes and Moderately Volatile Elements from Planetary Embryos and Early Venus, Earth and Mars. *Space Sci. Rev.*, 216, doi:10.1007/s11214-020-00701-x
- Leblanc, F., Martinez, A., Chaufray, J. Y., Modolo, R., Hara, T., Luhmann, J., et al (2018), On Mars's atmospheric sputtering after MAVEN's first Martian year of measurements. *Geophys. Res. Lett.*, 45, 4685–4691, doi:10.1002/2018GL077199
- Lemaire, J. (1974), The “Roche-limit” of ionospheric plasma and the formation of the plasmopause. *Planetary and Space Sci.*, 22, 757–766
- Lemaire, J. F. (2001), The formation of the light-ion trough and peeling off the plasmasphere. *J. Atmos. Sol.-Terr. Phys.*, 63, 1285–1291
- Lemaire, J., & Schunk, R.W. (1992), Plasmaspheric wind. *J. Atmos. Terr. Phys.* 54, 467–477, doi:10.1016/0021-9169(92)90026-H
- Li, K., Wei, Y., André, M., Eriksson, A., Haaland, S., Kronberg, E. A., et al. (2017), Cold ion outflow modulated by the solar wind energy input and tilt of the geomagnetic dipole. *J. Geophys. Res.*, 122, 10,658–10,668. doi:10.1002/2017JA024642
- Liao, J., Kistler, L. M., Mouikis, C. G., Klecker, B., & Dandouras, I. (2015), Acceleration of O⁺ from the cusp to the plasma sheet. *J. Geophys. Res.*, 120, 1022–1034, doi:10.1002/2014JA020341
- Lin, M.-Y., Ilie, R., & Glocer, A. (2020), The contribution of N⁺ ions to Earth's polar wind. *Geophys. Res. Lett.*, 47, e2020GL089321, doi:10.1029/2020GL089321
- Lundin, R., Lammer, H. & Ribas, I. (2007), Planetary Magnetic Fields and Solar Forcing: Implications for Atmospheric Evolution. *Space Sci. Rev.*, 129, 245–278, doi:10.1007/s11214-007-9176-4
- Maes, L., Maggiolo, R., De Keyser, J., Dandouras, I., Fear, R. C., Fontaine, D. & Haaland, S. (2015), Solar illumination control of ionospheric outflow above polar cap arcs. *Geophys. Res. Lett.*, 42, 1304–1311. doi:10.1002/2014GL062972
- Maggiolo, R., Echim, M., De Keyser, J., Fontaine, D., Jacquy, C., & Dandouras, I. (2011), Polar cap ion beams during periods of northward IMF: Cluster statistical results. *Ann. Geophys.*, 29, 771–787, doi:10.5194/angeo-29-771-2011
- Mall, U. A., Christon, S. P., Kirsch, E., & Gloeckler, G. (2002), On the solar cycle dependence of the N⁺/O⁺ content in the magnetosphere and its relation to atomic N and O in the Earth's exosphere. *Geophys. Res. Lett.*, 29, doi:10.1029/2001GL013957
- Marcucci, M. F., et al. (2004), Energetic magnetospheric oxygen in the magnetosheath and its response to IMF orientation: Cluster observations. *J. Geophys. Res.*, 109, doi:10.1029/2003JA010312
- Mende, S., Heeterdks, H., Frey, H. U., Stock, J. M., Lampton, M., Geller, S. P., Abiad, R., Siegmund, O. H. W., Habraken, S., Renotte, E., Jamar, C., Rochus, P., Gerard, J.-C., Sigler, R.,

- & Lauche, H. (2000), Far ultraviolet imaging from the IMAGE spacecraft. 3. Spectral imaging of Lyman- α and OI 135.6 nm. *Space Sci. Rev.*, *91*, 287–318, doi:10.1023/A:1005292301251
- Mitchell, D., Jaskulek, S., Schlemm, C. et al. (2000), High energy neutral atom (HENA) imager for the IMAGE mission. *Space Sci Rev*, *91*, 67–112, doi:10.1023/A:1005207308094
- Nilsson, H. (2011), Heavy ion energization, transport, and loss in the Earth's magnetosphere. *The Dynamic Magnetosphere*, edited by: Liu, W. and Fujimoto, M., doi:10.1007/978-94-007-0501-2_17, IAGA, Springer
- Nilsson, H., Waara, M., Arvelius, S., Marghitsu, O., Bouhram, M., Hobara, Y., Yamauchi, M., Lundin, R., Rème, H., Sauvaud, J.-A., Dandouras, I., Balogh, A., Kistler, L. M., Klecker, B., Carlson, C. W., Bavassano-Cattaneo, M. B., & Korth, A. (2006), Characteristics of high altitude oxygen ion energization and outflow as observed by Cluster: a statistical study. *Ann. Geophys.*, *24*, 1099–1112, doi:10.5194/angeo-24-1099-2006
- Nilsson, H., Waara, M., Marghitsu, O., Yamauchi, M., Lundin, R., Rème, H., Sauvaud, J.-A., Dandouras, I., Lucek, E., Kistler, L. M., Klecker, B., Carlson, C. W., Bavassano-Cattaneo, M. B., & Korth, A. (2008a), An assessment of the role of the centrifugal acceleration mechanism in high altitude polar cap oxygen ion outflow. *Ann. Geophys.*, *26*, 145–157, doi:10.5194/angeo-26-145-2008
- Nilsson, H., Waara, M., Marghitsu, O., Yamauchi, M., Lundin, R., Rème, H., Sauvaud, J.-A., Dandouras, I., Lucek, E., Kistler, L. M., Klecker, B., Carlson, C. W., Bavassano-Cattaneo, M. B., & Korth, A. (2008b), Transients in oxygen outflow above the polar cap as observed by the Cluster spacecraft. *Ann. Geophys.*, *26*, 3365–3373, doi:10.5194/angeo-26-3365-2008
- Nilsson, H., Barghouthi, I. A., Slapak, R., Eriksson, A. I., & André, M. (2012), Hot and cold ion outflow: Spatial distribution of ion heating. *J. Geophys. Res.*, *117*, doi:10.1029/2012JA017974
- Parks, G. K., Lee, E., Fu, S. Y., Fillingim, M., Dandouras, I., Cui, Y. B., Hong, J., & Rème, H. (2015), Outflow of low-energy O⁺ ion beams observed during periods without substorms. *Ann. Geophys.*, *33*, 333–344, doi:10.5194/angeo-33-333-2015
- Perreault, P., & Akasofu, S.-I. (1978), A study of geomagnetic storms. *Geoph. J. of the Royal Astronomical Soc.*, *54* (3), 547–573, doi:10.1111/j.1365-246X.1978.tb05494.x
- Peterson, W. K., Collin, H. L., Yau, A. W. & Lennartsson, O. W. (2001), Polar/Toroidal Imaging Mass-Angle Spectrograph observations of suprathermal ion outflow during solar minimum conditions. *J. Geophys. Res.*, *106*, 6059 – 6066, doi: 10.1029/2000JA003006
- Pierrard, V., Goldstein, G., André, N., Jordanova, V.K., Kotova, G.A., Lemaire, J.F., Liemohn, M.W., & Matsui, H. (2009), Recent progress in physics-based models of the plasmasphere. *Space Sci. Rev.*, *145*, doi: 10.1007/s11214-008-9480-7
- Ramstad, R., & Barabash, S. (2021), Do Intrinsic Magnetic Fields Protect Planetary Atmospheres from Stellar Winds? *Space Sci. Rev.*, *217*, doi:10.1007/s11214-021-00791-1
- Rème, H., Aoustin, C., Bosqued, J.M., Dandouras, I., et al. (2001), First multispacecraft ion measurements in and near the Earth's magnetosphere with the identical Cluster ion spectrometry (CIS) experiment. *Ann. Geophys.*, *19*, 1303–1354, doi: 10.5194/angeo-19-1303-2001

- Ribas, I., Guinan, E. F., Güdel, M., & Audard, M. (2005), Evolution of the solar activity over time and effects on planetary atmospheres. I. High-energy irradiances (1–1700 Å). *Astrophys. J.*, *622*, 680–694, doi:10.1086/427977
- Roelof, E. C. (1987), Energetic neutral atom image of a storm-time ring current. *Geophys. Res. Lett.*, *14*, 652–655, doi:10.1029/GL014i006p00652
- Schillings, A., Nilsson, H., Slapak, R., Yamauchi, M., & Westerberg, L.-G. (2017), Relative outflow enhancements during major geomagnetic storms – Cluster observations. *Ann. Geophys.*, *35*, 1341–1352, doi:10.5194/angeo-35-1341-2017
- Schillings, A., Nilsson, H., Slapak, R., Wintoft, P., Yamauchi, M., Wik, M. et al. (2018), O⁺ escape during the extreme space weather event of 4–10 September 2017. *Space Weather*, *16*, 1363–1376, doi:10.1029/2018SW001881
- Schillings, A., Slapak, R., Nilsson, H. et al. (2019), Earth atmospheric loss through the plasma mantle and its dependence on solar wind parameters. *Earth Planets Space*, *71*, 70, doi:10.1186/s40623-019-1048-0
- Schunk, R.W. (2000), Theoretical developments on the causes of ionospheric outflow. *J. Atmosph. Solar Terr. Phys.*, *62*, 399–420
- Servaites, J.C. (1977), pH Dependence of Photosynthesis and Photorespiration in Soybean Leaf Cells. *Plant Physiol*, *60*, 693–696, doi:10.1104/pp.60.5.693
- Shelley, E. G., Peterson, W. K., Ghielmetti, A. G., & Geiss, J. (1982), The polar ionosphere as a source of energetic magnetospheric plasma. *Geophys. Res. Lett.*, *9*, 941–944, doi:10.1029/GL009i009p00941
- Sibeck, D. G., McEntire, R. W., Lui, A. T. Y., Lopez, R. E., Krimigis, S. M., Decker, R. B., Zanetti, L. J., & Potemra, T. A. (1987), Energetic magnetospheric ions at the dayside magnetopause: Leakage or merging?. *J. Geophys. Res.*, *92*, 12097–12114, doi:10.1029/JA092iA11p12097
- Slapak, R., & Nilsson, H. (2018), The oxygen ion circulation in the outer terrestrial magnetosphere and its dependence on geomagnetic activity. *Geophys. Res. Lett.*, *45*, 12669–12676, doi:10.1029/2018GL079816
- Slapak, R., Schillings, A., Nilsson, H., Yamauchi, M., Westerberg, L.-G., & Dandouras, I. (2017), Atmospheric loss from the dayside open polar region and its dependence on geomagnetic activity: implications for atmospheric escape on evolutionary timescales. *Ann. Geophys.*, *35*, 721–731, doi:10.5194/angeo-35-721-2017
- Strangeway, R. J., Ergun, R. E., Su, Y.-J., Carlson, C. W., & Elphic, R. C. (2005), Factors controlling ionospheric outflows as observed at intermediate altitudes. *J. Geophys. Res.*, *110*, A03221, doi:10.1029/2004JA010829
- Stüeken, E. E., Som, S. M., Claire, M. et al. (2020), Mission to Planet Earth: The First Two Billion Years. *Space Sci. Rev.*, *216*, doi:10.1007/s11214-020-00652-3
- Torkar, K., Riedler, W., Escoubet, C. P., Fehringer, M., Schmidt, R., Grard, R. J. L., Arends, H., Rüdener, F., Steiger, W., Narheim, B. T., Svenes, K., Torbert, R., André, M., Fazakerley, A., Goldstein, R., Olsen, R. C., Pedersen, A., Whipple, E., & Zhao, H. (2001), Active spacecraft

potential control for Cluster – implementation and first results. *Ann. Geophys.*, *19*, 1289–1302, doi:10.5194/angeo-19-1289-2001

Vallat, C., et al. (2004), First comparisons of local ion measurements in the inner magnetosphere with energetic neutral atom magnetospheric image inversions: Cluster-CIS and IMAGE-HENA observations. *J. Geophys. Res.*, *109*, doi:10.1029/2003JA010224

Wei, Y., Fraenz, M., Dubinin, E., Woch, J., Lühr, H., Wan, W., Zong, Q.-G., Zhang, T. L., Pu, Z. Y., Fu, S. Y., Barabash, S., Lundin, R., & Dandouras, I. (2012), Enhanced atmospheric oxygen outflow on Earth and Mars driven by a corotating interaction region. *J. Geophys. Res.*, *117*, doi:10.1029/2011JA017340

Wilken, B., Daly, P. W., Mall, U., Aarsnes, K., Baker, D. N., Belian, R. D., Blake, J. B., Borg, H., Büchner, J., Carter, M., Fennell, J. F., Friedel, R., Fritz, T. A., Gliem, F., Grande, M., Kecskemety, K., Kettmann, G., Korth, A., Livi, S., McKenna-Lawlor, S., Mursula, K., Nikutowski, B., Perry, C. H., Pu, Z. Y., Roeder, J., Reeves, G. D., Sarris, E. T., Sandahl, I., Søraas, F., Woch, J., & Zong, Q.-G. (2001), First results from the RAPID imaging energetic particle spectrometer on board Cluster. *Ann. Geophys.*, *19*, 1355–1366, doi:10.5194/angeo-19-1355-2001

Wilson, G. R., Ober, D. M., Germany, G. A., & Lund, E. J. (2004), Nightside auroral zone and polar cap ion outflow as a function of substorm size and phase. *J. Geophys. Res.*, *109*, doi:10.1029/2003JA009835

Yamauchi, M. (2019), Terrestrial ion escape and relevant circulation in space. *Ann. Geophys.*, doi: 10.5194/angeo-37-1197-2019

Yamauchi, M., & Wahlund, J.-E. (2007), Role of the Ionosphere for the Atmospheric Evolution of Planets. *Astrobiology*, *7*, 783–800, doi:10.1089/ast.2007.0140

Yamauchi, M., & Slapak, R. (2018), Energy conversion through mass loading of escaping ionospheric ions for different Kp values. *Ann. Geophys.*, doi: 10.5194/angeo-36-1-2018

Yau, A., & M. André (1997), Sources of Ion Outflow in the High Latitude Ionosphere. *Space Sci. Rev.*, doi:10.1023/A:1004947203046

Yau, A. W., Peterson, W. K., & Shelley, E. G. (1988), Quantitative parametrization of energetic ionospheric ion outflow. *Geophys. Monogr. Ser.*, *44*, 211–217, doi:10.1029/GM044p0211

Yau, A. W., Whalen, B. A., Goodenough, C., Sagawa, E., & Mukai, T. (1993), EXOS D (Akebono) observations of molecular NO⁺ and N₂⁺ upflowing ions in the high-altitude auroral ionosphere. *J. Geophys. Res.*, *98*, 11205–11224, doi:10.1029/92JA02019